



MASTER THESIS 2010

Title: The Drilling Process: A Plantwide Control Approach	Subject (3-4 words): Drilling, optimization, plantwide, control
Author: Dag-Erik Helgestad	Carried out through: 12.01.2010 – 08.06.2010
Advisor: Professor Sigurd Skogestad Co-advisor: John-Morten Godhavn, Statoil ASA	Main report: 63 pages Appendices: 25 pages + CD-ROM
ABSTRACT	
Goal of work (key words):	
<p>The goal of this thesis is to study the drilling process and create a simplified model based on drilling literature. The model should be used to optimize the drilling process based on total drilling costs for a set of given conditions. Further, we want to identify the optimal controlled variables for the drilling process. The self-optimizing controlled variables are variables that give the minimum loss when the process is subject to disturbances.</p>	
Conclusions (key words):	
<p>An extensive literature search was performed, covering the drilling process and the challenges involved. A steady-state model of the drilling process was created and used to optimize the drilling process for given parameters and conditions. The optimization of the drilling process was analyzed separately for the active drilling operations and pipe connections and drilling trips.</p> <p>The optimal controlled variables were identified using the method of maximizing the minimum singular value, the null space method and the exact local method. The results corresponded well with each other, identifying the weight on bit and the topdrive power as the optimal single measurement controlled variables. Research on avoiding stick-slip conditions during drilling support the conclusion of operating with a varying drill string rotational speed. Combining measurements will give a lower loss, but the loss is small (approximately 1% of the active drilling time) and the complexity of the control structure will increase. The savings compared to a constant input policy were relatively low, approximately 1% of the active drilling time. However, the drilling process is very expensive, and any savings in drilling time will equal a substantial revenue.</p> <p>The time spent during pipe connection- and drilling trip procedures is identified as an important factor in the optimization of the drilling process. A simple dynamic pressure model was used to simulate the performance of a automated feedback pressure control structure involving PI controllers. The control structure was able to perform the required procedures while keeping the bottom hole pressure within a pressure window of ± 5 bar.</p>	
<p>I declare that this is an independent work according to the exam regulations of the Norwegian University of Science and Technology</p>	
<p style="text-align: center;">Date and signature:</p>	

Preface

This master thesis was written during the spring of 2010 as a compulsory part of the study program leading to a Master of Science (sivilingeniør) degree in Chemical Engineering at the Norwegian University of Science and Technology (NTNU). The thesis work has allowed me to explore the field of drilling engineering and study the drilling process, while simultaneously increase my knowledge in the field of process control. I have had a great learning profit and I am sure that I will benefit of this thesis work in the future.

I would like to thank my supervisor for this project, Professor Sigurd Skogestad at the Process Systems Engineering group at NTNU, Trondheim, for support and guidance throughout the semester. Equally, I wish to thank my co-supervisor at Statoil ASA, John-Morten Godhavn, who originally proposed the project and has been a valuable asset for advice. I would also like to extend my gratitude to PhD student Ramprasad Yelchuru at the Process Systems Engineering group at NTNU, for taking the time to explain and help me understand the exact local method.

I would like to thank my fellow students Elisabeth Hyllestad, Martin Buus Jensen and Anders Haukvik Røed for keeping a good spirit and healthy, fun atmosphere at our office. It has been helpful to discuss our projects together and I very much enjoyed your company at coffee breaks.

Last but definitely not least, I would like to thank my parents, Riitta and Dag Helgestad. Your love and support (both moral and financial) has been an greatly appreciated throughout my years as a student.

Dag-Erik Helgestad
Trondheim, June 2010

Contents

List of Figures	vii
List of Tables	ix
List of Abbreviations	xi
1 Introduction	1
1.1 Motivation	1
1.2 Aim and Scope of the Thesis	2
2 Background	5
2.1 The Drilling Process	5
2.1.1 Managed Pressure Drilling (MPD)	6
2.2 Introduction to Numerical Optimization	8
2.3 Control Structure Design (Plantwide Control)	9
2.3.1 Local Analysis	11
2.3.2 Maximum Scaled Gain (Minimum Singular Value) Method	12
2.3.3 Null Space Method	13
2.3.4 Exact Local Method	14
2.4 PID Controller Design	15
3 Steady-State Drilling Model	17
3.1 Drilling Model Equations	17
3.1.1 The Rate of Penetration	17
3.1.2 Topdrive Torque and Power	19
3.1.3 Bottom Hole Cleaning	19
3.1.4 Bottom Hole Pressure	21
3.2 Parameters	23
3.2.1 Parameters Relationships	23
3.3 Drilling Model Results	24
4 Optimization and Active Constraint Control	25
4.1 Degrees of Freedom (DOF)	25
4.2 Objective Function: The Cost of Drilling	26
4.2.1 Bit Wear	27
4.2.2 Operating Modes	28
4.3 Operational Constraints	29
4.4 Optimization Results	30
4.5 Active Constraints	31
4.6 Unconstrained Optimization	31

5	Self-Optimizing Controlled Variables	33
5.1	Process Gains and Disturbances	34
5.2	Maximum Scaled Gain (Minimum Singular Value) Method	35
5.3	Null Space Method	36
5.4	Exact Local Method	37
5.5	Pairing of Variables	40
5.6	Discussion	40
5.7	Stick-Slip Phenomenon	42
6	Pressure Control and Automation	45
6.1	Pressure Control Structure	46
6.2	Pipe Connections and Drilling Trips	47
6.2.1	Automation with Controllers	48
6.3	Dynamic Pressure Model	49
6.4	Simulations	51
6.4.1	Controller Design	51
6.4.2	Results	51
6.5	Discussion: Model Predictive Control (MPC)	55
7	Conclusions and Further Work	57
7.1	Conclusions	57
7.1.1	Optimal Controlled Variables	57
7.1.2	Pressure Control & Automation	58
7.2	Further work	59
	Bibliography	60
	A Nomenclature	65
	B Miscellaneous Calculation Matrices	67
	C Solving the Exact Local Method for a Multivariable Case	69
	D Results of the Exact Local Method	71
	E MATLAB files	75

List of Figures

- 1.1 The drilling rig Deepwater Horizon burning and sinking in the Gulf of Mexico . . . 2
- 2.1 Schematic of an offshore drilling rig 6
- 2.2 Typical control system hierarchy in a chemical plant 10
- 2.3 Loss imposed by keeping a constant set point for the controlled variable 11
- 2.4 Block diagram of a control structure with measurement combinations as controlled variables 13
- 4.1 Plots of the objective function $J(u, d)$ vs the weight on bit (WOB) and the drill string RPM 32
- 4.2 Surface plot of the objective function $J(u, d)$ versus the WOB and the drill string RPM 32
- 5.1 Plot of maximum loss versus the number of combined measurements 38
- 5.2 Plot of maximum loss of optimal measurement combinations versus the magnitude of disturbances 39
- 5.3 Plot of maximum loss of poor measurement combinations versus the magnitude of disturbances 39
- 5.4 Plot of friction torque as a function of rotational speed of the drill string 43
- 6.1 Schematic of a well, with the drilling mud circulation system 46
- 6.2 Block diagram of the pressure control structure 47
- 6.3 MATLAB Simulink switch block 48
- 6.4 Block diagram of the pressure control structure with controllers for the main mud pump flow rate and drill bit position 49
- 6.5 Bottom hole pressure, main pump pressure, choke pressure and choke pressure set point responses to a drilling trip simulation 52
- 6.6 Close-up of the bottom hole pressure response in Figure 6.5 52
- 6.7 Valve position response to a drilling trip simulation 53
- 6.8 Main pump and drill bit flow rate response to a drilling trip simulation 53
- 6.9 Back pressure pump flow rate and choke flow response to a drilling trip simulation 54
- 6.10 Drill bit vertical position response to a drilling trip simulation 54
- 6.11 Illustration of the MPD well control system with control hierarchy 55

List of Tables

2.1	Summary of Important Notation	9
3.1	Penetration Rate Equation Parameters	18
3.2	Drilling Model Parameters	23
3.3	Drilling Model Inputs	24
3.4	Drilling Model Outputs	24
4.1	Manipulated Variables (MV's) in the Drilling Process	26
4.2	Recommended Tooth-Wear Parameters for Rolling-Cutter Bits	28
4.3	Operational Constraints in the Drilling Process	30
4.4	Nominal Optimal Values	30
4.5	Details About the Optimization	30
4.6	Active Constraints in the Drilling Process	31
5.1	Expected Disturbances	34
5.2	Implementation Errors	35
5.3	Optimal Variation, Implementation Errors and Expected Optimal Span	35
5.4	Minimum Singular Value Results	36
5.5	Optimal Controlled Variables	38
6.1	Dynamic Pressure Model Parameters	50
7.1	Optimal Controlled Variables	58
A.1	Nomenclature	65
D.1	Optimal Combinations of 6 Measurements	71
D.2	Optimal Combinations of 5 Measurements	71
D.3	Optimal Combinations of 4 Measurements	72
D.4	Optimal Combinations of 3 Measurements	73
D.5	Optimal Combinations of 2 Measurements	74
E.1	List of MATLAB Files	75

List of Abbreviations

BHA	Bottom hole assembly
BHP	Bottom hole pressure
BOP	Blow-out preventer
CV	Controlled variable
DOF	Degree(s) of freedom
MPC	Model Predictive Control
MPD	Managed Pressure Drilling
MV	Manipulated variable
MWD	Measurement While Drilling
PI	Proportional-integral (controller)
PID	Proportional-integral-derivative (controller)
QP	Quadratic program
RCD	Rotating Control Device
ROP	Rate of penetration
RPM	Revolutions per minute
RTO	Real-time Optimizer
SQP	Sequential quadratic programming
WOB	Weight on bit

Chapter 1

Introduction

1.1 Motivation

According to the International Energy Agency (IEA), the world energy demand is expected to increase by 44% from 2006 to 2030.[1] At the same time, most of the easily-attained petroleum reserves are already exploited. The result is that the petroleum industry is facing technical challenges in most areas of the upstream industry. The remaining reservoirs are smaller, deeper and in more remote locations than the typical reservoir of the previous decades. There is a need for accurate, cost-effective drilling systems capable of drilling complex wells with increased demands on pressure control.

The process of drilling a well is very expensive, as it involves hiring a drilling rig and crew for the duration of drilling the well. It is therefore important to drill the well as fast as possible in order to minimize the cost. The drillers are highly experienced and aim to drill fast and safe, while keeping within a set of boundaries and handling upsets. However, the drilling process involves coordinating a lot of machinery and making quick decisions with the possibility of severe consequences. The catastrophic blowout on the drill rig Deepwater Horizon in the Gulf of Mexico in April 2010 clearly showed the magnitude of the potential dangers. The blowout led to the burning and sinking of the drill rig (see Figure 1.1), and an oil leak with huge environmental impact. Naturally, the situation became the focus of world press and political agendas, as well as having enormous economical consequences for the responsible companies.

Many of the decisions made on the rig floor require extremely good knowledge of the various effects in the drilling process, and they should be made faster than what is possible for a human. Also, the decisions are often based on experience and out-dated industry standards which are not necessarily optimal for each and every purpose. Therefore, the drilling process has great potential for increased automation and optimization in terms of process control.

The downstream industry is highly dependent on good process control, as the refinery product specifications are controlled very tightly. The application of properly designed control structures and properly tuned controllers has increased the regularity and thus the profit margins of refinery products. It is desirable to analyze the drilling process using a plantwide control approach, in order to determine the optimal variables to control during drilling. The resulting control



Figure 1.1: The drill rig Deepwater Horizon burning and sinking in the Gulf of Mexico, April 21, 2010. *Photo: U.S. Coast Guard. Used according to license cc by-sa 2.0 Generic, cf. <http://www.flickr.com/photos/uscgd8/4542937668/>*

structure should provide near-optimal operation even when it is subject to disturbances in drilling parameters, such as varying formation strength, density or pressure.

The implementation of various new technology such as Managed Pressure Drilling (MPD) have increased the performance and safety of drilling systems. However, such additions are often implemented independently of the existing drilling operation system, so there is little coordination between e.g. the drilling system and the pressure control system. A fully integrated control structure for the drilling process would increase the efficiency and coordination between both operators and machinery.

1.2 Aim and Scope of the Thesis

The goal of this thesis is to analyze the drilling process with a plantwide control approach. The work involves:

- Studying the drilling process to better understand the objective and the importance of the various process variables.
- Creating a simplified steady-state drilling model in MATLAB based on drilling literature (Chapter 3).
- Identifying an objective function and constraints for the drilling process, and optimizing the process with respect to the degrees of freedom (Chapter 4).
- Identifying the optimal (self-optimizing) controlled variables (Chapter 5). The self-optimizing controlled variables are variables that give the minimum loss when the process is subject to expected disturbances.

The steady-state optimization and identification of optimal controlled variables assumes that the time spent making pipe connections and drilling trips is constant. However, pipe connections and drilling trips are recognized as important operations in terms of minimizing the total drilling time. Therefore, an additional study of the performance of feedback pressure control structure is performed (Chapter 6).

Chapter 2

Background

This section will introduce the process of drilling a well for petroleum production, including the equipment used and challenges that are faced. The first section will describe the traditional setup of a drilling rig, while the purpose and design of a Managed Pressure Drilling (MPD) system is described in the succeeding section. The last sections include an introduction to numerical optimization and an introduction to control structure design (plantwide control), as well as a description of PID controllers.

2.1 The Drilling Process

The drilling of wells into petroleum reserves is performed by a drilling rig, such as illustrated in Figure 2.1. The drilling rig in the figure is a jacket platform used in offshore drilling operations. The drill string with the drill bit at the end is rotated by the topdrive, an electric motor at the top end of the drill string. The topdrive is attached to a hook in the derrick, making it possible to raise and lower the drill string by the drawworks (hoisting system). While drilling, the drill string is lowered due to the weight of the string and the progress of the drill bit. As the position of the topdrive reaches the bottom of the derrick, a new stand of drill pipe added and the hook position is moved to the top of the new connection. Each stand of pipe is approximately 27 meters in length, so a typical penetration rate of 15 m/hr will require a new connection approximately every other hour.[2]

Although not clearly illustrated in Figure 2.1, the drilling rig contains a mud circulation system. The drilling mud is pumped through the drill string to the bottom of the well and returns to the surface through the well annulus. The cuttings are separated from the returning mud in *shale shakers*, and the mud is sent back to mud tanks on the drill rig. The main functions of the drilling mud are to:

- Provide hydrostatic pressure to the well to prevent formation fluids from entering the well during drilling.
- Transport the rock cuttings away from the bit (to ensure efficient drilling) and back to the surface through the well annulus.

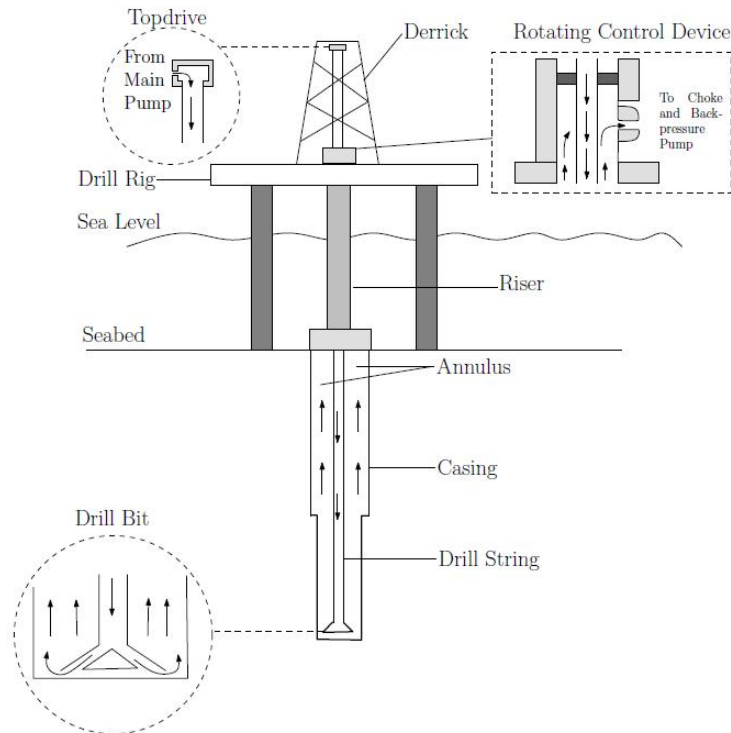


Figure 2.1: Offshore drilling rig (jacket platform). Drilling mud flows from the main pump through the drill string, out of the bit and back up in the well annulus. The mud transports the rock cuttings out of the well, and also provides hydrostatic pressure to the borehole.[2]

- Keep the drill bit cool and clean during operation.

Drilling muds also have special properties allowing them to suspend the cuttings while drilling is paused and the mud is stationary. Various drilling muds have even more specific functions, such as sealing permeable formations, controlling corrosion and facilitating cementing, but these effects will not be covered in this thesis.

2.1.1 Managed Pressure Drilling (MPD)

Figure 2.1 of the example drilling rig shows that the top of the annulus is sealed off by a rotating control device (RCD). The RCD is a part of a newer, more sophisticated drilling technology called Managed Pressure Drilling (MPD). In conventional drilling, the mud return is *open*, meaning it returns to atmospheric pressure. With the implementation of a RCD, the returning mud must exit through a choke valve, and the valve opening may be controlled by the drillers. This system provides a means for controlling the pressure profile in the well annulus, which is very important factor in achieving effective drilling. It is important to keep the pressure profile within the pressure window, which depends on the characteristics of the formation.

The pressure in the well must be above the collapse pressure of the borehole, to prevent the bore hole from catastrophically closing in due to the differential pressure acting from outside to inside of the well. Similarly it is important to keep the pressure below the fracturing pressure of the

bore hole, in order to prevent hydraulic fracture of the rock formation. Another important aspect of well pressure control is to prevent uncontrolled influx of reservoir fluids or loss of drilling mud into the formation. In the case of too low pressure, formation fluids may flow into the annulus and be driven towards the surface by the pressure gradient. This phenomenon is called a drilling kick, and is often encountered during drilling. In the worst case, a kick may lead to a surface blowout, causing large financial losses and possible damages to environment and human lives. If the well pressure is higher than the formation pressure, the drilling mud will flow into the porous reservoir and possibly clog up the pores. Drilling mud is fairly expensive, so losses are certainly undesirable, but the loss of mud may also restrict the production from that part of the reservoir.

The pressure in the annulus is mainly affected by the hydrostatic weight of the mud, but also the pressure that arises due to friction losses when the mud is circulated. The RCD and choke valve make it possible for the drillers to set a pressure at the top of the annulus by manipulating the choke valve opening. The annulus pressure profile will be affected by the pressure at the top, thus facilitating control of the bottom hole pressure (BHP). In addition to the choke valve, the top side of the annulus is also connected to a back pressure pump. This pump is included to help the choke valve provide the required pressure, as the choke valve naturally is restricted to its fully closed and fully open positions.

Being able to apply a pressure at the top of the annulus reduces the risk of drilling kicks leading to a blowout, as the kick may be countered by increasing the choke pressure. The advantage is that we are able to drill *underbalanced*, in other words with a bottom-hole pressure that is lower than the formation pressure. Underbalanced drilling increases the rate of penetration, eliminates formation damage because no mud is forced into the formation, reduces lost circulation and eliminates differential sticking. However, it is critical that the pressure control system is reliable.

Several procedures during drilling operations have significant effects on the annulus pressure. Each time a pipe connection is made, the main pump is disconnected and circulation stops. The pressure term due to friction is thereby lost. Changing the drill bit or other failures require a full retraction of the drill string from the well, called a drilling trip. The volume of the well is increased, leading to a lower mud height and pressure. The opposite (a pressure surge) is experienced when inserting the drill string back into the well. Similar effects of vertical movement of the drill string are experienced in offshore drilling due to wave motion (heave).

It is clear that accurate control of the annulus pressure profile is important during all aspects of the drilling process. In Managed Pressure Drilling (MPD) control structures, the bottom hole pressure (the pressure at the drill bit) or the shoe pressure (the pressure at the bottom of the casing, above the openhole section) is usually chosen as the controlled variable. However, the downhole pressures are not easily measured. Information from the bottom of the well is traditionally sent to the surface by pulses in the mud (mud-pulse telemetry). These signals are not available when the mud circulation rate is low or stopped completely, e.g. during pipe connections. Instead, advanced hydraulic models have been used to estimate the downhole pressures. Stamnes [2] studied the estimation of the bottom hole pressure (BHP) using adaptive observers. For the course of this thesis we however assume a wired drill string with exact measurement of the bottom hole pressure.

2.2 Introduction to Numerical Optimization

Optimization problems are seen in various applications, such as stock portfolios, chemical processes and transportation logistics. Optimization is also present in various levels of typical industry companies, from management to design to operation. The purpose of any optimization is to find the values of the variables corresponding to the best possible value of a given objective function. An optimization problem function can be linear or non-linear, and may be subject to constraints. A general optimization problem can be defined as follows:

$$\begin{aligned} \text{Minimize (or maximize): } J &= f(x) & (2.1) \\ \text{Subject to: } g(x) &\leq 0 \\ h(x) &= 0 \end{aligned}$$

In Equation 2.2, J represents the objective function, which is a function of variable(s) x . The optimization problem may be subject to inequality constraints $g(x)$ and equality constraints $h(x)$.

Different optimization methods have been developed in order to solve problems such as above. In the case where both objective function and constraints are linear functions of the variables, the optimization becomes a linear programming problem. If either objective function or constraints are non-linear functions of the variables, the problem is non-linear and more sophisticated methods are required to solve the problem.

One of the most popular and robust methods for non-linear optimization is the sequential quadratic programming (SQP) algorithm. The SQP algorithm handles both equality and inequality constraints, and is reduced to Newton's method for finding a point where the gradient of the objective is zero if the problem is unconstrained. The method constructs and solves a local model of the optimization problem and yields a step towards the solution of the original problem. The SQP algorithm uses a quadratic model for the objective function and linear models for the constraints. This is called a *quadratic program* (QP). The quadratic programs are solved sequentially, by minimizing the Lagrangian function with the linear approximation of the constraints in order to reach the optimum for the problem.[3] The optimum is defined by the Karush-Kuhn-Tucker conditions, a generalization of the method of Lagrangian multipliers to inequality constraints.[4]

The Karush-Kuhn-Tucker conditions are analogous to the condition that the gradient of the objective function must be zero at optimum, modified to take constraints into account. The conditions are based on the method of Lagrange multipliers, with the inclusion of inequality constraints rather than being restricted to equality constraints. The Lagrange function for a constrained optimization problem is presented in Equation 2.2.

$$L(x, \lambda) = f(x) + \sum \lambda_{g,i} g_i(x) + \sum \lambda_{h,i} h_i(x) \quad (2.2)$$

The vector λ is the concatenation of vectors λ_g and λ_h , and is the vector of Lagrange multipliers. The KKT conditions are presented in Equations 2.3 through 2.7:

$$\nabla_x L(x, \lambda) = 0 \quad (2.3)$$

$$\lambda_{g,i} g_i(x) = 0 \quad \forall i \quad (2.4)$$

$$g(x) \leq 0 \quad (2.5)$$

$$h(x) = 0 \quad (2.6)$$

$$\lambda_{g,i} \geq 0 \quad (2.7)$$

Equation 2.3 represents the condition of a zero gradient of the Lagrangian function, while Equation 2.4 represents the complementary slackness. Equations 2.5 and 2.7 require that the inequalities and equalities constraints are met, while Equation 2.7 requires that the Lagrangian multipliers associated with the inequality constraint functions are positive.[4]

2.3 Control Structure Design (Plantwide Control)

Control structures in the chemical industry are often organized in a hierarchy as illustrated in Figure 2.2.[5] As indicated in the figure, the two bottom layers are parts of the control structure, while the layers above provide the operational setpoints for the process. In order to design a control structure one must carefully analyze the process at hand. A lot of work may be put into designing and tuning controllers, but the control structure itself may be far from optimal for its purpose. This section will present the procedures of Skogestad et al. [5, 6, 7, 8, 9, 10] for control structure design and selection of self-optimizing controlled variables. A summary of important notation is presented in Table 2.1.

Table 2.1: Summary of Important Notation

u	Unconstrained degree of freedom (MV)
y	Measurement (including u 's)
z	Controlled variable (CV)
n_u	# of u 's
n_z	# of CV's ($n_z = n_u$)
n_y	# of y 's ($n_y \geq n_z$)
$J(u, d)$	Cost function to be minimized
$J_{opt}(d)$	Optimal value of J
$L = J(u, d) - J_{opt}(d)$	Loss

The plantwide control approach to a control structure design problem is based on *top-down* and *bottom-up* procedures. The *top-down* analysis is used to determine the controlled outputs, while the *bottom-up* procedures are used to select measurements and manipulated variables as well as determine a control configuration. The procedures are summarized below. [5]

Top-down:

1. Identify a cost function J for the process and identify operational constraints.
2. Identify the degrees of freedom available to the process.
3. Analyze the solution for optimal operation for various disturbances, with the purpose of determining the primary controlled variables (CV's) which, when kept at a constant set point, indirectly minimize the cost.

Bottom-up:

1. *Regulatory control:* Identify additional variables to be measured and controlled, and suggest pairing with manipulated inputs.

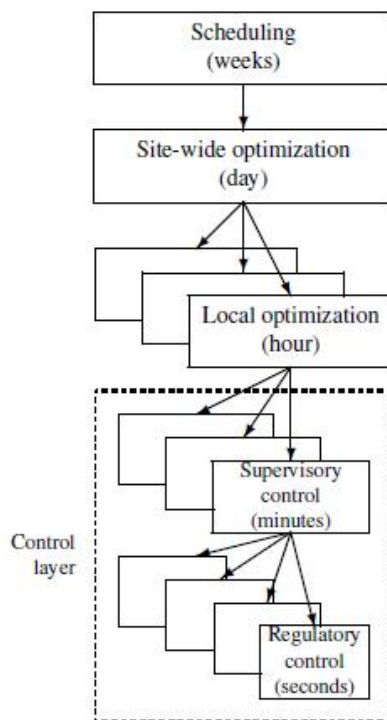


Figure 2.2: Typical control system hierarchy in a chemical plant.[5]

2. *Supervisory control*: Propose a configuration for a supervisory control layer (decentralized, MPC).
3. *On-line optimization*: Determine whether a real-time optimizer (RTO) is needed, or whether constant setpoints are sufficient.

The *top-down* procedures with selection of the controlled variables is the most critical part of the plantwide control approach. After optimizing with respect to the objective function J and the operational constraints, we get the nominal optimal values for the manipulated variables or inputs (u), and the measurements (y). The next step is to determine the optimal controlled variables (CV's), also denoted as z . First, active constraints must be controlled to ensure optimal operation. One degree of freedom (manipulated variable) is consumed for control of each active constraint. Further, we want to choose the best possible CV's to control with the remaining manipulated variables. We want to choose CV's that, when controlled at a constant set point, give minimal loss when the process is subject to disturbances. The optimal CV's are therefore called *self-optimizing* controlled variables. The idea is illustrated in Figure 2.3, where z_1 is a better controlled variable than z_2 .

The self-optimizing controlled variables may be determined by performing so-called *brute-force* analyses. This involves selecting various combinations of controlled variables, introducing expected disturbances and calculating the loss. However, in most cases we have many measurements to choose from but only a few manipulated variables, which leads to very many combinations of CV's. Therefore, we use mathematical methods to determine the best controlled variables. We will perform a local analysis of the loss function to explain the theory.

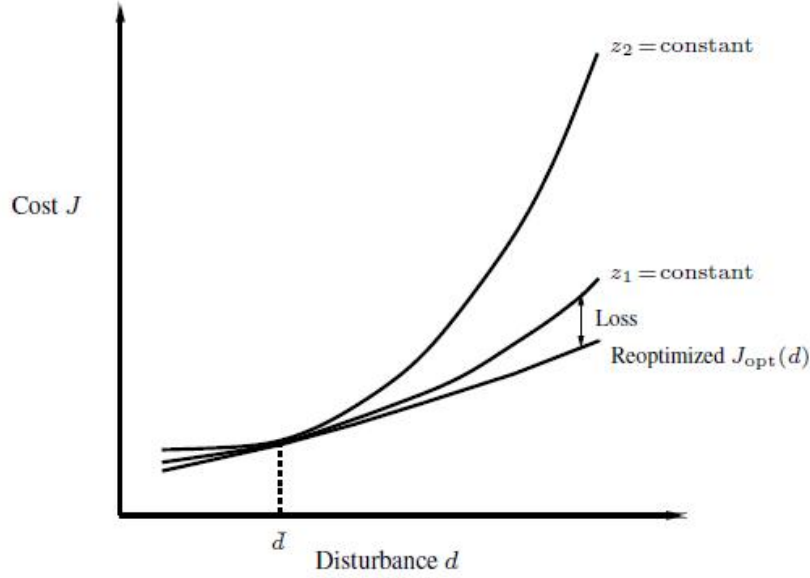


Figure 2.3: Loss imposed by keeping a constant set point for the controlled variable. In this case z_1 is a better *self-optimizing* controlled variable than z_2 . [5]

2.3.1 Local Analysis

The loss function is the difference between the cost function $J(u, d)$ and the re-optimized cost function $J_{opt}(u, d)$, where d represents a disturbance to the system. The cost function $J(u, d)$ is assumed to be twice differentiable, and the optimization problem is considered to be unconstrained. Any active constraints should have been removed (both the measurement and one degree of freedom) from further analysis as described above. We want to determine which variables are best to control by the remaining manipulated variables.

The objective function may be expressed as a local second-order Taylor series expansion around the nominal optimal point of operation. This is shown in Equation 2.8.

$$J(u, d) = J_{opt}(u, d) + [J_u \quad J_d]^T \begin{bmatrix} \Delta u \\ \Delta d \end{bmatrix} + \frac{1}{2} \begin{bmatrix} \Delta u \\ \Delta d \end{bmatrix}^T \begin{bmatrix} J_{uu} & J_{ud} \\ J_{du} & J_{dd} \end{bmatrix} \begin{bmatrix} \Delta u \\ \Delta d \end{bmatrix} \quad (2.8)$$

where $\Delta u = u - u_{opt}$ and $\Delta d = d - d_{opt}$. We recognize that the gradient of the objective function with respect to the manipulated variables (J_u) is equal to zero at the unconstrained optimum. For a given disturbance d ($\Delta d = 0$), the loss function may be written as Equation 2.9.

$$L = J - J_{opt} = \frac{1}{2} (u - u_{opt})^T J_{uu} (u - u_{opt}) \quad (2.9)$$

Introducing $\tilde{z} = J_{uu}^{1/2} (u - u_{opt})$, we may reduce the notation to Equation 2.10. $\|\tilde{z}\|_2$ is the 2-norm, or maximum singular value of \tilde{z} .

$$L = \frac{1}{2} \|\tilde{z}\|_2^2 \quad (2.10)$$

2.3.2 Maximum Scaled Gain (Minimum Singular Value) Method

The controlled variables (z) are chosen as a subset of the available measurements (y). The controlled variables (z) may be expressed as a function of the manipulated variables (u) and the disturbances (d) as shown in Equation 2.11.

$$z = Gu + G_d d \quad (2.11)$$

Assuming that the disturbance d is fixed ($\Delta d = 0$), we may write $z - z_{opt} = G(u - u_{opt})$. Equation 2.12 shows how $z - z_{opt}$ can be written as a sum of an optimization error e_{opt} and an implementation error n .

$$z - z_{opt} = z - r + r - z_{opt} = n + e_{opt}(d) \quad (2.12)$$

The optimization error is the difference between the optimal value z_{opt} and the set point for the controller r (the nominal optimal value). The implementation error is the difference between the controller set point and the actual value of z . The implementation error is due to imperfect control, or due to incorrect measurements, which often are a factor in real systems. The absolute value of $z - z_{opt}$ is called the *expected optimal span* of the measurements, and is denoted $span(z)$.

For a multivariable case, z and u are vectors. According to Skogestad & Postlethwaite [5], the outputs are scaled with respect to their optimal span by multiplication with the output scaling matrix $S_1 = \text{diag}\{1/span(z_i)\}$. The resulting scaled outputs are shown in Equation 2.13, where $G' = S_1 G$.

$$z' - z'_{opt} = S_1 G(u - u_{opt}) = G'(u - u_{opt}) \quad (2.13)$$

Using $(u - u_{opt}) = G'^{-1}(z' - z'_{opt})$ and Equation 2.10, we write Equation 2.14.

$$L = \frac{1}{2} \|J_{uu}^{1/2} G'^{-1}(z' - z'_{opt})\|_2^2 \quad (2.14)$$

The scaled output deviation $z' - z'_{opt}$ has a magnitude of less than unity due to the scaling. Therefore, the maximum value of the 2-norm $\|z' - z'_{opt}\|_2$ is unity. The maximum expected loss for a multivariable case may then be expressed as in Equation 2.15.[5]

$$\begin{aligned} L_{max} &= \max_{\|z' - z'_{opt}\|_2 \leq 1} \frac{1}{2} \|J_{uu}^{1/2} G'^{-1}(z' - z'_{opt})\|_2^2 \\ &= \frac{1}{2} \bar{\sigma}^2(J_{uu}^{1/2} G'^{-1}) = \frac{1}{2} \frac{1}{\underline{\sigma}^2(G' J_{uu}^{-1/2})} \end{aligned} \quad (2.15)$$

The maximum of the 2-norm $\|\tilde{z}\|_2$ is given by the induced 2-norm $\|J_{uu}^{1/2} G'^{-1}\|_2$, which is equal to the maximum singular value $\bar{\sigma}(J_{uu}^{1/2} G'^{-1})$. The last equality is given by the relationship between the maximum and minimum singular values, as shown in Equation 2.16.

$$\bar{\sigma}(A^{-1}) = 1/\underline{\sigma}(A) \quad (2.16)$$

From Equation 2.15 we can deduce that it is optimal to choose measurements that maximize the minimum singular value $\underline{\sigma}(G' J_{uu}^{-1/2})$, where $G' = S_1 G$.

2.3.3 Null Space Method

We have considered z as a subset of the available measurements y . However, if we use linear combinations of measurements y to form various z 's, we have an infinite number of potential controlled variables available.[5, 10] We express z as shown in Equation 2.17. A block diagram of a control structure with measurement combinations is presented in Figure 2.4.

$$z = Hy \quad (2.17)$$

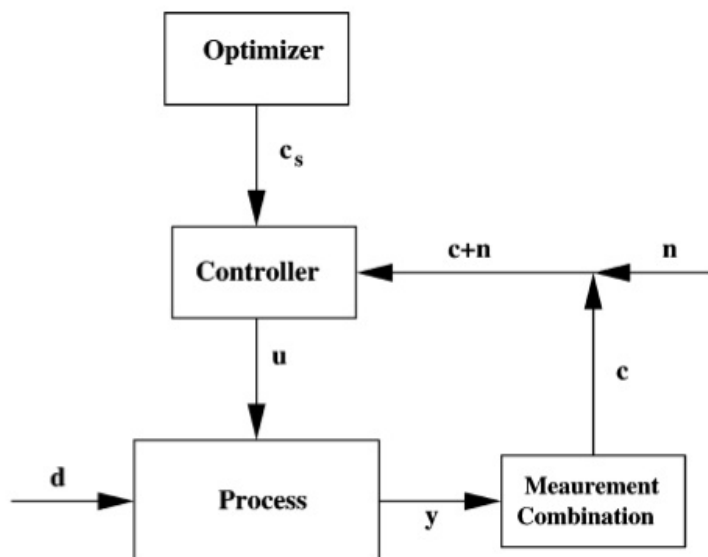


Figure 2.4: Block diagram of a control structure with measurement combinations as controlled variables.[9] Note: The controlled variables are denoted c in the figure, while this thesis uses notation z .

The re-optimized values of the measurements (y_{opt}) depend on the disturbance that is introduced on the system. They also depend on the implementation error (see Equation 2.12), but for this case we assume that the implementation errors are negligible. We may express this relationship as shown in Equation 2.18. The matrix F may be viewed as the gain from the disturbance d to the optimal variation of the measurements.

$$\Delta y_{opt} = F \Delta d \quad (2.18)$$

Optimally, we want z_{opt} to be independent of the disturbance d ($\Delta z_{opt} = 0 \cdot \Delta d$). Combining Equation 2.17 with Equation 2.18, we get Equation 2.19.

$$\Delta z_{opt} = HF \Delta d \quad (2.19)$$

In order to achieve optimal constant set points ($z_{opt} = 0$), we require that $HF = 0$. In other words, H must be in the left null space of F . The null space of F has dimension $n_y - n_d$ so we

must require $n_z = n_u \leq n_y - n_d$. The last inequality then states that we must choose to combine $n_y \geq n_u + n_d$ measurements for the controlled variables z . The optimal controlled variables (measurement combinations) may be determined using Equation 2.20.

$$z = Hy = \text{null}(F) \cdot y \quad (2.20)$$

2.3.4 Exact Local Method

The exact local method also considers optimal linear combinations of measurements, but takes implementation errors into account. For a constant set point policy, Halvorsen et. al.[9] showed that the optimal variation in the manipulated variables is given by Equation 2.21.

$$\Delta u_{opt} = (u - u_{opt}) = -J_{uu}^{-1} J_{ud} \Delta d \quad (2.21)$$

The expression in Equation 2.21 is obtained from Equation 2.8 by applying a given disturbance ($\Delta d = 0$) and recognizing that $J_u = 0$ at optimum. The optimal variation in the measurements (y) may then be expressed as in Equation 2.22

$$\Delta y_{opt} = G \Delta u + G_d \Delta d = -(G J_{uu}^{-1} J_{ud} - G_d) \Delta d = F \Delta d \quad (2.22)$$

The F matrix is the disturbance sensitivity matrix from disturbances d to measurements y at the nominal optimum, same as in Equation 2.18. The control variables are a linear combination of the measurements, as shown in Equation 2.23.

$$z = Hy \quad (2.23)$$

The deviation in manipulated variables may also be expressed in terms of the controlled variables, as shown in Equations 2.24 through 2.26. Δz_{opt} represents the optimal variation of the measurements, while Δz represents the implementation errors. Δz_s is neglected because we assume a constant set point policy.

$$(u - u_{opt}) = (HG)^{-1}(z - z_{opt}) = (HG)^{-1}(\Delta z - \Delta z_{opt}) \quad (2.24)$$

$$\Delta z_{opt} = H \Delta y_{opt} = HF \Delta d \quad (2.25)$$

$$\Delta z = \Delta z_s - n = -n = -Hn \quad (2.26)$$

We introduce the magnitudes of the disturbances d and implementation errors n in diagonal scaling vectors W_d and W_n as shown below.

$$\begin{aligned} \Delta d &= W_d d' \\ n &= W_n n' \end{aligned}$$

where d' and n' are vectors with:

$$\left\| \begin{bmatrix} d' \\ n' \end{bmatrix} \right\|_2 \leq 1$$

Re-writing Equation 2.24, we get Equation 2.27.

$$(u - u_{opt}) = (HG)^{-1}H [FW_d \ W_n] \begin{bmatrix} d' \\ n' \end{bmatrix} \quad (2.27)$$

We define the matrix \tilde{F} as follows:

$$\tilde{F} = [F \ W_d \ W_n]$$

Inserting Equation 2.27 into the loss function in Equation 2.10 we get Equation 2.28 for the loss.

$$L = \frac{1}{2} \|J_{uu}^{1/2}(HG)^{-1}H\tilde{F}\|_2^2 \quad (2.28)$$

For the case of a full matrix H , the problem in Equation 2.28 may be re-written as the quadratic programming problem in Equation 2.29.[8, 11]

$$\min_H \|H\tilde{F}\|_2 \quad (2.29)$$

$$\text{subject to: } HG = J_{uu}^{1/2}$$

2.4 PID Controller Design

A *proportional – integral – derivative* (PID) controller has three terms, one proportional to the error (e), one proportional to the integral of the error and one proportional to the derivative of the error. The output of the PID controller is the value of the manipulated input $u(t)$. The PID controller equation is presented in Equation 2.30.

$$u(t) = K_P e(t) + K_I \int_0^t e(\tau) d\tau + K_D \frac{de(t)}{dt} \quad (2.30)$$

K_P , K_I and K_D are the tuning parameters of the controller, and are called the *proportional* gain, *integral* gain and *derivative* gain, respectively. Only PI controllers are used in the work with this thesis, in order to facilitate simpler tuning. The PI controller equation is simply Equation 2.30 without the last term involving the derivative action. Thus, we are left with only two tuning parameters, K_P and K_I .

Chapter 3

Steady-State Drilling Model

A simplified steady-state drilling model was created in MATLAB in order to simulate the drilling process. This section will explain the equations behind the drilling model, and explain the various assumptions that were made. The assumptions are based upon drilling literature search performed as part of the thesis work. The MATLAB files for the model are attached in Appendix E.

3.1 Drilling Model Equations

3.1.1 The Rate of Penetration

The rate of penetration (ROP) is the speed in at which the drill string and bit are propelled into the formation. The ROP depends on several factors, including the weight on bit (WOB), the rotational speed of the bit, the pressure gradient at the bottom of the well and the hydraulic jet impact force of the drilling fluid. The ROP may also be viewed as a manipulated variable itself, while e.g. treating the WOB as the dependent variable. However, this report has focused on the treating the ROP as a measurement.

Bourgoyne and Young [12, 13] have presented a complex model for the rate of penetration, expressed as a function containing 8 multiplied terms (Equation 3.1).

$$R = f_1 f_2 f_3 f_4 f_5 f_6 f_7 f_8 \quad (3.1)$$

The factors $f_1 - f_8$ represent various effects on the rate of penetration (R in Equation 3.1) by formation strength, depth, WOB, drill string rotational speed, differential pressure, jet impact force of the mud, etc. The factor f_1 models the effects of formation strength and bit type on the rate of penetration, and is constant for given drilling conditions and bit type. The effect of increasing formation strength due to normal compaction with depth is included in f_2 , while f_3 models the effect of under-compaction in abnormally pressured formations. The factors f_2 and f_3 are also constant for a given formation. The factor f_4 models the effect of over- or underbalance on the penetration rate, and is presented in Equation 3.2. The equation is modified from the

original equation by Bourgoyne and Young [12, 13], where it is a function of the mud density. The factors f_5 and f_6 are related to the weight on bit (WOB) and rotational speed of the bit, and are presented in Equations 3.3 and 3.4. The effect of tooth wear is modeled in factor f_7 , but is assumed to be constant for a steady-state model. The factor f_8 is presented in Equation 3.5 and models the effect of the hydraulic jet impact force of the drilling mud on the penetration rate. The equations were originally published using engineering units, but have been altered to SI units for the thesis work.

$$f_4 = e^{a_4(p_f - p_{bh})} \quad (3.2)$$

$$f_5 = \left[\frac{\left(\frac{W}{d_b}\right) - \left(\frac{W}{d_b}\right)_t}{71.4 - \left(\frac{W}{d_b}\right)_t} \right]^{a_5} \quad (3.3)$$

$$f_6 = \left(\frac{N}{60}\right)^{a_6} \quad (3.4)$$

$$f_8 = \left(\frac{F_j}{4482}\right)^{a_8} \quad (3.5)$$

W represents the weight on bit (WOB) in metric tons while N represents the rotational speed of the bit in revolutions per minute (RPM). The diameter of the drill (and thus also the well at the given depth) is expressed as d_b . $(W/d_b)_t$ represents the threshold WOB per bit diameter that is required to penetrate the given surface, and is therefore dependent on the formation characteristics. p_f represents the formation pressure at the bottom of the well in *bar*, while p_{bh} represents the bottom hole pressure in the wellbore. F_j represents the hydraulic jet impact force in *Newton*.

The constant terms $f_1 - f_3$ and f_7 were combined in one constant, R_0 . This constant represents the formation drillability in units *m/hr*. The resulting equation for the ROP is given in Equation 3.6. The exponents a_4 , a_5 , a_6 and a_8 were chosen based on typical values found in literature, and are presented in Table 3.1.[13]

Table 3.1: Penetration Rate Equation Parameters

Parameter	a_4	a_5	a_6	a_8
Value	0.01	1	0.7	0.3

$$R = R_0 e^{0.01(p_f - p_{bh})} \left[\frac{\left(\frac{W}{d_b}\right) - \left(\frac{W}{d_b}\right)_t}{71.4 - \left(\frac{W}{d_b}\right)_t} \right] \left(\frac{N}{60}\right)^{0.7} \left(\frac{F_j}{4482}\right)^{0.3} \quad (3.6)$$

Equation 3.6 shows that the rate of penetration increases linearly with increasing W (WOB), while the increase is less than linear with N , the rotational speed of the bit. The gain in ROP

by increased rotational speed N will be less prominent at higher values of N . Both responses make physical sense, though some may argue that the rate of penetration should decrease at higher values of WOB. The reason for such a physical response is widely believed to be a result of insufficient bottom-hole cleaning, and not a direct consequence of an increase in WOB.[13] Insufficient hole cleaning will result in re-grinding of cuttings that are not quickly transported away from the drill bit, leading to a less-than-optimal rate of penetration. However, we assume perfect hole cleaning conditions and expect a response similar to that of Equation 3.6.

3.1.2 Topdrive Torque and Power

The torque and power of the topdrive are useful measurement to monitor during the drilling process, and may be feasible variables for controlling the process. The torque that is needed to rotate the drill string is the product of the force F_c and the length of the arm that the force is acting on, in this case the radius of the drill string. The force F_c can be expressed as the product of the specific cutting force k_c and the area of the drilled surface, as shown in Equation 3.7, where d_s denotes the diameter of the drill string.

$$T = F_c \frac{d_s}{2} = k_c \frac{d_b^2 d_s \pi}{8} \quad (3.7)$$

The specific cutting force k_c depends on the formation strength, but also on the weight on bit. It is assumed that the specific cutting force can be modeled as a product of a parameter k_c^0 which only depends on the formation characteristics, multiplied with the WOB. This is shown in Equation 3.8.

$$k_c = k_c^0 W \quad (3.8)$$

The topdrive power (in kW) can be calculated from the torque (T) as shown in Equation 3.9.

$$P = \frac{2 \pi N T}{60\,000} \quad (3.9)$$

3.1.3 Bottom Hole Cleaning

As mentioned in Section 2.1, one of the purposes of the drilling mud is to transport the cuttings away from the bit and up to the surface through the well annulus. It is very important to ensure sufficient transport of the cuttings, otherwise the drill bit will keep grinding the cuttings that accumulate at the bottom of the well. This will lead to a lower rate of penetration and thus less efficient drilling.

The circulation rate and properties of the drilling mud determine its capacity of transporting the cuttings. First, the slip velocity of the particles must be determined, which is dependent on the geometry and density of the cuttings. The slip velocity for Newtonian fluids in *creeping flow*, i.e. very low Reynolds numbers (< 0.1), may be calculated using Stoke's law. Choosing realistic values for the annulus velocity, mud density, viscosity and the diameters of the drill string and well, an estimate of the Reynolds number may be made as shown Equation 3.11. The hydraulic

diameter of an annulus may be calculated using Equation 3.10.

$$d_H = \frac{\pi(d_b^2 - d_s^2)}{\pi(d_b + d_s)} = d_b - d_s \quad (3.10)$$

$$N_{Re} = \frac{\rho_f v_a d_H}{\mu} = \frac{1400 \text{ kg/m}^3 \cdot 0.7 \text{ m/s} \cdot (0.254 \text{ m} - 0.100 \text{ m})}{0.02 \text{ Pa}\cdot\text{s}} = 7546 \quad (3.11)$$

From Equation 3.11 it is clear that Stoke's law can not be used. For Reynolds numbers over 0.1, empirically determined friction coefficients must be used. The friction coefficient in this case is defined in Equation 3.12,

$$f = \frac{F}{A E_K} \quad (3.12)$$

where

- F = force exerted on the particle due to viscous drag,
- A = characteristic area of the particle, and
- E_K = kinetic energy per unit volume.[13]

The force F is the difference between the weight and buoyancy of the particle, defined by Equation 3.13. The particle diameter is denoted d_p , while ρ_s and ρ_f denote the particle density and the effective mud density, respectively. The kinetic energy E_K is defined by Equation 3.14, where v_{sl} is the particle slip velocity.

$$F = F_g - F_{bo} = (\rho_s - \rho_f) g (\pi d_p^3 / 6) \quad (3.13)$$

$$E_K = \frac{1}{2} \rho_s v_{sl}^2 \quad (3.14)$$

Assuming the particles are spherical, the characteristic area is given as $A = \pi d_p^2 / 4$. Combining the equations gives Equation 3.15 for the friction factor.

$$f = \frac{4}{3} g \frac{d_p}{v_{sl}^2} \frac{\rho_s - \rho_f}{\rho_f} \quad (3.15)$$

Several correlations have been proposed in order to let the slip velocity equations apply for non-Newtonian fluids, such as drilling muds. Moore [14, 13] proposed that for Reynolds numbers above 300, the flow around the particle is fully turbulent and the friction factor becomes constant at a value of about 1.5. Chien [15, 13] recommends the use of 1.72 for the friction coefficient for Reynolds numbers above 100. Though slightly different for lower Reynolds numbers, the different correlations seems to agree rather closely for turbulent flows. Thus, using Moore's correlation and solving Equation 3.15 for the slip velocity, we get Equation 3.16.

$$v_{sl} = \sqrt{\frac{8}{9} g d_p \frac{\rho_s - \rho_f}{\rho_f}} \quad (3.16)$$

The effective transport velocity v_T of the cuttings is defined as the difference between the annulus mud velocity and the slip velocity of the particles. The expression is shown in Equation 3.17. Assuming that the mud flow through the bit (q_{bit}) is equal to the flow of mud from the main pump (q_{in}), the annulus flow velocity is expressed as in Equation 3.18. A_a represents the cross-sectional area of the well annulus.

$$v_T = v_a - v_{slip} \quad (3.17)$$

$$v_a = \frac{q_{bit}}{A_a} = \frac{4 q_{in}}{\pi (d_b^2 - d_s^2)} \quad (3.18)$$

The transport velocity can be used to calculate the fraction of cuttings (x_c) in the mud that is flowing in the well annulus, since it can also be expressed as a function of the rate of cuttings as shown in Equation 3.19.[13]

$$v_T = \frac{q_s}{A_a x_c} \quad (3.19)$$

The feed of cuttings per second (q_s) is determined by the ROP (R) as shown in Equation 3.20, and the fraction of solids in the mud return can be calculated by re-organizing Equation 3.19 as shown in Equation 3.21.

$$q_s = \frac{R}{3600} A_b = \frac{R}{3600} \pi \frac{d_b^2}{4} \quad (3.20)$$

$$x_c = \frac{q_c}{A_a v_T} \quad (3.21)$$

The effective density of the returning mud is dependent on the fraction of cuttings, and is calculated using Equation 3.22.

$$\rho_f = x_c \rho_s + (1 - x_c) \rho_m \quad (3.22)$$

The transport velocity v_T must be greater than zero in order for the cuttings to be transported out of the well. A negative v_T means that the slip velocity is higher than the annulus velocity, resulting in an accumulation of cuttings at the bottom of the well. While a small, positive v_T in theory would bring the cuttings to the surface, this would result in a very high percentage of cuttings in the mud and significantly increase the mud density, which in turn would lead to a higher bottom-hole pressure and thus less favorable drilling conditions (refer to Equations 3.2 and 3.6).

3.1.4 Bottom Hole Pressure

All measurements from the bottom of the well are in practice rather difficult to obtain. The measurements may be sent to the top by mud pulse telemetry, but this technology is ineffective during times of lost circulation and when the mud circulation rate is low. Mud-pulse telemetry requires a minimum flow rate of approximately 600-1000 *liter/min*. The measurements are updated only 1-10 times per minute and experience a couple of seconds of delay as they are transmitted to

the surface. Underbalanced drilling also imposes several other challenges to mud pulse telemetry, as gas that is introduced to reduce the equivalent mud density causes signal attenuation and drastically reduces the ability to transmit data through the mud. However, as mentioned in Section 2.1.1, we assume we have a wired drill pipe providing accurate measurements of the bottom hole pressure.

The measurement of the bottom hole pressure was modeled using simple fluid mechanics. The flow of mud through the well annulus to the surface may be used to determine the pressure profile. The annulus flow is assumed to be one-dimensional and we neglect other momentum effects that may be experienced due to the rotation of the drill string. We also assume that the drilling fluid is incompressible.

At steady-state and applying the assumptions above, the Navier-Stokes equations are reduced to Equation 3.23. F represents the friction forces affecting the flow, z is the length coordinate along the path of the flow (positive direction upwards), while A_a represents the cross-sectional area of the annulus.

$$0 = -\frac{\partial p}{\partial z} - \frac{1}{A_a} \frac{\partial F}{\partial z} - \rho_f g \quad (3.23)$$

We assume the friction gradient $\partial F/\partial z$ is constant, and integrate Equation 3.23 from $z = -D$ to $z = 0$. D is the depth of the well in meters ($D > 0$). Further, we re-organize to get p_{bh} on the left side of the equation, and get Equation 3.24.

$$p_{bh} = p_c + \frac{1}{A_a} \frac{\partial F}{\partial z} D + \rho_f g D \quad (3.24)$$

The friction loss term is dependent on the geometry of the flow (in this case an annulus) and is difficult to calculate accurately. For this simple model, we assume that the annulus pressure drop due to friction is linearly dependent on the mud flow. For a mud flow of $1 \text{ m}^3/\text{min}$, we assume a 15 bar pressure drop, giving a friction parameter $\theta = \frac{15}{1/60} = 900 \text{ bar} \cdot \text{s}/\text{m}^3$. The final equation for the bottom-hole pressure measurement is shown in Equation 3.25.

$$p_{bh} = p_c + \theta q_{in} + \rho_f g D \quad (3.25)$$

The first term represents the choke pressure, in other words the pressure at the top of the annulus. The choke pressure term is only relevant for MPD systems that involve a sealed-off annulus (RCD) and choke valve. For conventional drilling with an open mud return, p_c is equal to the atmospheric pressure. The second term represents the pressure loss due to friction. The last term is the hydrostatic pressure from the annulus mud column, which is the also the dominant term in the expression.

3.2 Parameters

The various parameters in the drilling model are summarized in Table 3.2.

Table 3.2: Drilling Model Parameters

Parameter	Description	Value	Unit
d_b	Drill bit diameter	0.254	m
$(W/d_b)_t$	Threshold WOB per diameter	12.6	$tons/m$
d_s	Drill string diameter	0.10	m
d_p	Drilled particle diameter	0.005	m
θ	Annulus friction parameter	900	$kg/m^4 s$
D	Depth of well	3 000	m
ρ_m	Drilling mud density	1 400	kg/m^3
ρ_s	Cuttings density	2 700	kg/m^3
R_0	Formation drillability	5	m/hr
k_c^0	Formation cutting force parameter	100 000	$N/ton m^2$

3.2.1 Parameters Relationships

Several parameters in the model equations are related to the formation strength. In Section 5.1, disturbances are applied in order to determine the optimal variables for control in a self-optimizing structure. Treating the different parameters as individual disturbances, the system would be subject to more disturbances than there are measurements available. Such a scenario is undesirable, as it would be difficult for the control structure to respond. Additionally, such a model would not be realistic, as a disturbance in formation strength should affect all of the related parameters simultaneously.

Since this is a simplified model, the various parameters related to the formation strength were modeled as functions of the formation drillability R_0 . An increase in formation strength corresponds to a reduction in drillability. Similarly, the threshold WOB needed to penetrate the formation increases, so it is modeled as inversely proportional to R_0 as shown in Equation 3.26.

$$\left(\frac{W}{d_b}\right)_t \propto \frac{1}{R_0} \quad (3.26)$$

The topdrive torque and power should increase with increasing formation strength. Thus, the parameter k_c^0 is modeled as inversely proportional to the formation drillability R_0 . See Equation 3.27. The nominal value of k_c^0 was determined to give a realistic result for the topdrive power.

$$k_c^0 \propto \frac{1}{R_0} \quad (3.27)$$

It is emphasized that the relations described in the equations above are not based on exact empirical results or theoretical deduction, rather logical reasoning of a realistic scenario. While being a simplified model, they should be sufficient to provide reasonable responses for the various parameters to a disturbance in formation strength. It should also be emphasized that the drilling

model is not based on any specific scenario or field data, but should be interpreted as a simple model of a fictional drilling process.

3.3 Drilling Model Results

A steady-state model of the drilling process was created in MATLAB as a function accepting the various inputs (denoted u) and returning the values of the measurements (denoted y). The MATLAB files are attached in Appendix E. The inputs to the drilling model are presented in Table 3.3, and the output of the drilling model is presented in Table 3.4.

Table 3.3: Drilling Model Inputs

Input (u)	Description	Value	Unit
W	Weight on Bit (WOB)	30	<i>tons</i>
N	Drill string RPM	100	<i>min</i> ⁻¹
q_{in}	Main mud pump flow	40	<i>liter/s</i>
p_c	Choke pressure	10	<i>bar</i>

Table 3.4: Drilling Model Outputs

Measurement (y)	Description	Value	Unit
R	Rate of penetration (ROP)	17.61	<i>m/hr</i>
T	Topdrive torque	29.92	<i>kNm</i>
P	Topdrive power	313.36	<i>kW</i>
x_c	Fraction of cuttings in mud	0.79	<i>%</i>
p_{bh}	Bottom hole pressure	461	<i>bar</i>

Chapter 4

Optimization and Active Constraint Control

This section will provide an analysis and overview of the various factors affecting the cost of the drilling process in order to identify the objective function for the optimization problem. The degrees of freedom for optimization of the process will be presented. An equation describing the cost of drilling (objective function) is derived, and the operational constraints will be identified. Finally, the nominal optimal values of both manipulated variables and measurements are determined, as well as the active constraints at optimum.

4.1 Degrees of Freedom (DOF)

In general, a degree of freedom (DOF) is a single scalar number describing a micro-state of a system. The system is then completely described by all its degrees of freedom. For process design, the number of steady-state DOF's is the number of variables (parameters) that must be specified to completely define the process. The degrees of freedom can be calculated by subtracting the number of specified variables (equations) from the number of process variables, as shown in Equation 4.1.

$$N_{SS} = N_{var} - N_{SV} \quad (4.1)$$

N_{var} represents the number of process variables, and N_{SV} represents the number of specified variables (equations). However, counting equations is not a very efficient procedure. The steady-state degrees of freedom for a process may also be determined by counting the manipulated variables N_{MV} and subtracting the variables with no steady-state effect and the process specifications. The degrees of freedom in the drilling process involve all manipulated variables (MV's) available to the driller. They are recapitulated in Table 4.1. We assume that Managed Pressure Drilling (MPD) is available, thus allowing us to use the choke pressure (p_c) as a degree of freedom.

In MPD systems, the choke pressure p_c is set by the choke valve and back pressure pump associated with the rotating control device (RCD). The choke valve is used to control the pressure,

Table 4.1: Manipulated Variables (MV's) in the Drilling Process

MV (u)	Description	Unit
W	Weight on Bit (WOB)	<i>tons</i>
N	Drill string RPM	min^{-1}
q_{in}	Main mud pump flow	<i>liter/s</i>
p_c	Choke pressure	<i>bar</i>

but its range is limited to the fully opened and fully closed positions of the valve. The back pressure pump can apply additional pressure in order to lift the range of the choke valve to the appropriate level. However, the choke pressure is treated directly as a manipulated variable in this thesis as it represents one degree of freedom in the process.

4.2 Objective Function: The Cost of Drilling

In order to study the optimization of the drilling process it is critical to identify the objective function of the problem. The drilling is usually performed by a contractor and paid on a per-day basis. Thus, the major concern when optimizing the drilling process is naturally to reduce the lease time. The same applies to companies that own their own drill rigs and employ their own operators, as a faster drilling time may allow the rig to be used for other tasks sooner. We assume that the costs of energy, drill bits and other equipment is negligible in comparison to the per-day cost of keeping the rig in operation.

The cost of drilling may be represented as in Equation 4.2. J represents the total cost of drilling, C_f represents a fixed cost for leasing the drilling rig while C_{var} represents the operational costs per hour. The total time of leasing the drilling rig consists of the drilling time (t_d), the time spent making pipe connections (t_c), and the total trip time (t_t).

$$J = C_f + C_{var}(t_d + t_c + t_t) \quad (4.2)$$

The drilling time may be expressed as the total depth of the well in meters (D), divided by the average rate of penetration (R) in m/hr . See Equation 4.3.

$$t_d = \frac{D}{R} \quad (4.3)$$

The total time spent making connections to the drill string is a function of both the depth and the connection time (t_c^0). The relationship is shown in Equation 4.4. It is assumed that each pipe connection is 27 meters long, so $\frac{D}{27}$ pipe connections must be made in to reach the desired depth of the well.

$$t_c = t_c^0 \frac{D}{27} \quad (4.4)$$

The total trip time is difficult to predict. Many trips are necessary and planned in order to change the drill bit and install well casing, but other unexpected conditions or disturbances may also cause problems to the equipment and cause a trip. We assume that the total trip time may

be expressed as a product of the time spent on a single trip multiplied by the number of trips. The number of trips required for bit changes is the drilling time (t_d) divided by the lifetime of the bit (t_d^0). The lifetime of the bit depends on the operating conditions and wear the bit is exposed to. In addition, a constant number of trips (1 every 1000 meters) are assumed for the installation of casing and other purposes. The total trip time is expressed in Equation 4.5

$$t_t = t_t^0 \left(\frac{t_d}{t_d^0} + \frac{D}{1000} \right) = t_t^0 \left(\frac{D}{R t_d^0} + \frac{D}{1000} \right) \quad (4.5)$$

Combining Equations 4.2 to 4.5, the cost function of the drilling process may be expressed as Equation 4.6.

$$J = C_f + C_{var} \left(\frac{D}{R} + t_c^0 \frac{D}{27} + t_t^0 \left(\frac{D}{R t_d^0} + \frac{D}{1000} \right) \right) \quad (4.6)$$

Naturally, it is desirable to perform the drilling as fast as possible. At first glance, one may expect this to be ambiguous with maximizing the rate of penetration (R). However, the drill bit wear is affected by the operating conditions and is an important factor in optimizing the drilling.

4.2.1 Bit Wear

The drill bit must be changed when either the teeth or the bearings are completely worn out.[13]. We assume that the bit teeth wear out before the bearings, so the bit lifetime is equivalent to the time needed to completely wear down the teeth. According to Bourgoynne et. al. [13], the bit tooth wear may be modeled as shown in Equation 4.7

$$\frac{dh}{dt} = \frac{1}{\tau_H} \left(\frac{N}{60} \right)^{H_1} \left[\frac{\left(\frac{W}{d_b} \right)_m - 71.4}{\left(\frac{W}{d_b} \right)_m - \left(\frac{W}{d_b} \right)} \right] \left(\frac{1 + H_2/2}{1 + H_2 h} \right) \quad (4.7)$$

where

- h = fractional tooth height that has been worn away,
- t = time, hours,
- $H_1, H_2, (W/d_b)_m$ = constants,
- τ_H = formation abrasiveness constant, hours.

As in Equation 3.6 on page 18, W and N represent the weight on bit and rotational speed of the drill string, respectively. The recommended values for H_1 , H_2 and $(W/d_b)_m$ from various rolling-cutter rock bit classes are presented in Table 4.2.[13] $(W/d_b)_m$ represents the maximum WOB per diameter of drill bit that should be used. For the course of this work, the drill bit has been assumed to be a class 3-1 bit.

$(W/d_b)_m$ in Table 4.2 has units lb/in . When converted to metric units, we get $(W/d_b)_m = 178.6 \text{ tons}/m$. A bit diameter of 0.254 m (10 in.) gives $W_m = 45.36 \text{ tons}$ for the maximum WOB.

Table 4.2: Recommended Tooth-Wear Parameters for Rolling-Cutter Bits [13]

Bit Class	H_1	H_2	$(W/d_b)_m$
1-1 to 1-2	1.90	7	7.0
1-3 to 1-4	1.84	6	8.0
2-1 to 2-2	1.80	5	8.5
2-3	1.76	4	9.0
3-1	1.70	3	10.0
3-2	1.65	2	10.0
3-3	1.60	2	10.0
4-1	1.50	2	10.0

Defining a tooth wear parameter J_2 as in Equation 4.8, we may rewrite Equation 4.7 as shown in Equation 4.9.

$$J_2 = \left[\frac{\left(\frac{W}{d_b}\right)_m - \left(\frac{W}{d_b}\right)}{\left(\frac{W}{d_b}\right)_m - 71.4} \right] \left(\frac{60}{N}\right)^{H_1} \left(\frac{1}{1 + H_2/2}\right) \quad (4.8)$$

$$\int_0^{t_d^0} dt = J_2 \tau_H \int_0^{h_f} (1 + H_2 h) dh \quad (4.9)$$

Integrating Equation 4.9 we get Equation 4.10.

$$t_d^0 = J_2 \tau_H (h_f + H_2 h_f^2 / 2) \quad (4.10)$$

We assume that the same bit (class 3-1) is used consequently, so there will be no changes in parameters. By collecting the constants in one single time constant K , we get Equation 4.11.

$$t_d^0 = K \left[\frac{\left(\frac{W}{d_b}\right)_m - \left(\frac{W}{d_b}\right)}{\left(\frac{W}{d_b}\right)_m - 71.4} \right] \left(\frac{60}{N}\right)^{1.7} \quad (4.11)$$

K may be regarded as a *bit lifetime constant* and is naturally dependent on the strength and abrasiveness of the drilled formation. The bit lifetime constant K will be reduced as a result of an increase in formation strength, and is thus modeled as proportional to the drillability R_0 (Equation 4.12).

$$K \propto R_0 \quad (4.12)$$

The value of K was set to 75 hours by trial and error to give a realistic value for the bit lifetime of approximately 15 hours.

4.2.2 Operating Modes

In addition to the operating conditions, Equation 4.6 on page 27 shows that the drilling process costs are highly dependent on the non-drilling times (t_c^0 and t_t^0). In fact, it may be easier to divide

the process into two specific operating modes: One for the actual drilling, and one for the pipe connections and drilling trips. This is due to the nature of the plantwide control approach of this project. The same objectives are not applicable to both *modes* of the process. During connections and trips, pressure control is the only relevant control objective. The design and performance of the pressure control system during pipe connections and trips is studied in Chapter 6.

During the actual drilling operation, the specific connection time (t_c^0) and trip time (t_t^0) may be assumed constant. Thus, the second term in the main brackets of Equation 4.6 and the last term regarding the trip time are regarded as constant. With respect to minimizing the cost function, constant terms are irrelevant and may be neglected. The resulting equation is presented in Equation 4.13.

$$\min J = \min \left(\frac{D}{R} + t_t^0 \frac{D}{R t_d^0} \right) \quad (4.13)$$

The trip time constant t_t^0 was assumed to be 10 hours. The other terms (penetration rate R and the bit-lifetime t_d^0) are dependent on the drilling operating conditions and are part of the optimization problem. The total well depth D is constant and could be removed, but was kept in the objective function in order to give it the more comprehensible units of time (hours). The depth D was set to 3 000 meters.

4.3 Operational Constraints

There are several constraints that need to be taken into account during drilling, both for measurements and for inputs. The most important constraints are the pressure constraints, as described in Section 2.1.1. The bottom hole pressure must be controlled within its limits very accurately. We assume the bottom hole pressure is constrained between 470 and 480 *bar* for a depth of 3 000 meters.

The weight on bit (WOB) is constrained by the threshold WOB (Table 3.2) on page 23 and the maximum WOB per diameter $(W/d_b)_m$ (Table 4.2 on page 28). We assume that the rotational speed of the drill string has an upper constraint of 200 RPM, as values above this would most likely cause problems for the equipment. The specifications of the topdrive motor naturally provide physical limits for the torque and power. However, we assume that the topdrive has sufficient capacity to operate at the optimal conditions.

The mud circulation rate may be altered in order to affect various measurements, such as the pressure profile, the fraction of cuttings in the returning mud, or the penetration rate. A high mud circulation rate will provide a higher jet impact force through the nozzles of the drill bit. However, increasing the mud flow rate beyond a certain point will eventually increase the frictional losses in both drill string and annulus. In turn, this will reduce the jet impact force at the bit, thus reducing the rate of penetration and increasing the drilling costs.[13] A high mud circulation rate also increases the risk of mud loss if the well is overbalanced. In order to take these considerations into account in the optimization problem, the mud flow rate was constrained at a maximum of 50 *liter/s*. The operational constraints are recapitulated in Table 4.3.

Table 4.3: Operational Constraints in the Drilling Process

Constraint	Lower Bound	Upper Bound	Unit
W	3.2	45.4	<i>tons</i>
N	0	200	<i>min</i> ⁻¹
q_{in}	0	50	<i>liter/s</i>
p_{bh}	470	480	<i>bar</i>

4.4 Optimization Results

The optimization of the drilling process was carried out in MATLAB using the *fmincon* function for non-linear constrained minimization. The *active-set* algorithm for the *fmincon* function uses a sequential quadratic programming (SQP) method, solving a quadratic program (QP) at each iteration and updating an estimate of the Hessian of the Lagrangian function.[16]

The scripts and functions that were used are attached in Appendix E. The nominal optimal values for the objective function, the manipulated variables and the measurements are presented in Table 4.4. Some information about the optimization routine is presented in Table 4.5.

Table 4.4: Nominal Optimal Values

Obj. fun.	Nom. opt.	Unit
J	249.09	<i>hours</i>
MV's	Nom. opt.	Unit
W	33.1	<i>tons</i>
N	100	<i>min</i> ⁻¹
q_{in}	50	<i>liter/s</i>
p_c	10.3	<i>bar</i>
Measurements	Nom. opt.	Unit
R	20.5	<i>m/hr</i>
T	33	<i>kNm</i>
P	344	<i>kW</i>
x_c	0.7	%
p_{bh}	470.0	<i>bar</i>

Table 4.5: Details About the Optimization

Number of iterations	24
Function Evaluations	131
First order optimality measure	$3.8 \cdot 10^{-4}$
Active inequalities	2

The Hessian of the Lagrangian function (refer to Section 2.2) at optimum is presented below.

$$\nabla_{uu}^2 L(u, \lambda) = 10^4 \cdot \begin{bmatrix} 0.1005 & -0.0006 & -0.1483 & 0.5960 \\ -0.0006 & 0.0086 & 0.0063 & -0.0218 \\ -0.1483 & 0.0063 & 0.2223 & -0.8908 \\ 0.5960 & -0.0218 & -0.8908 & 3.5719 \end{bmatrix}$$

The active constraints in the optimization are the lower bottom hole pressure constraint and the upper mud circulation rate constraint.

4.5 Active Constraints

It is important to control the constraints that are active at the optimum to ensure optimal operation. This holds for any type of process. As an example, consider a chemical plant producing product A that is sold with a purity requirement of 95%. The purity specification constraint will likely be active at optimal operation, because it is uneconomic to produce the product with a higher purity. A purity that is higher than the required specification would mean the company is selling a higher value product for a lesser price. In order to ensure optimal operation of the plant when disturbances to the process occur, it is important to control the purity by a manipulated variable (e.g. heat applied to separation process, or feed of a specific reactant).

The active constraints in the drilling process model are the bottom hole pressure (p_{bh}) and the mud circulation rate (q_{in}). The control of each active constraint consumes one manipulated variable (MV). We assume the bottom hole pressure is controlled using the choke pressure (p_c) as described in Section 2.1.1, and thus omit the choke pressure and the mud flow rate from further analysis.

4.6 Unconstrained Optimization

The bottom hole pressure and the mud circulation rate are omitted from the optimization, and are specified at their constrained values shown in Table 4.6.

Table 4.6: Active Constraints in the Drilling Process

Active Constraint	Value	Unit
q_{in}	50	<i>liter/s</i>
p_{bh}	470	<i>bar</i>

The remaining optimization problem is unconstrained. The Hessian matrix of the objective function (J_{uu}) at the unconstrained optimum is presented below.

$$\nabla^2 J(u) = J_{uu} = \begin{bmatrix} 1.8816 & 0.1159 \\ 0.1159 & 0.0222 \end{bmatrix}$$

Graphical representations of the objective function versus the two unconstrained degrees of freedom, the weight on bit (WOB) and rotational speed of the drill string, are presented in Figures 4.1a and 4.1b. A 3-dimensional surface plot of the objective function is presented in Figure 4.2.

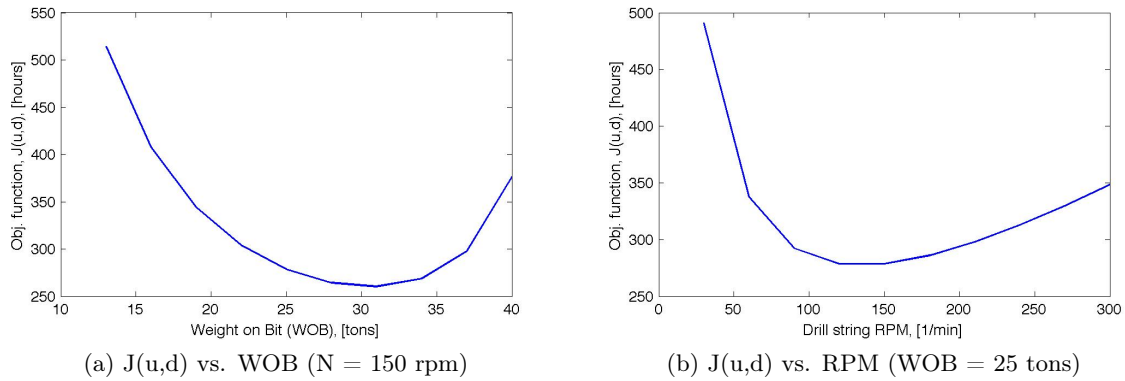


Figure 4.1: Plots of the objective function $J(u,d)$ vs the weight on bit (WOB) and the drill string RPM.

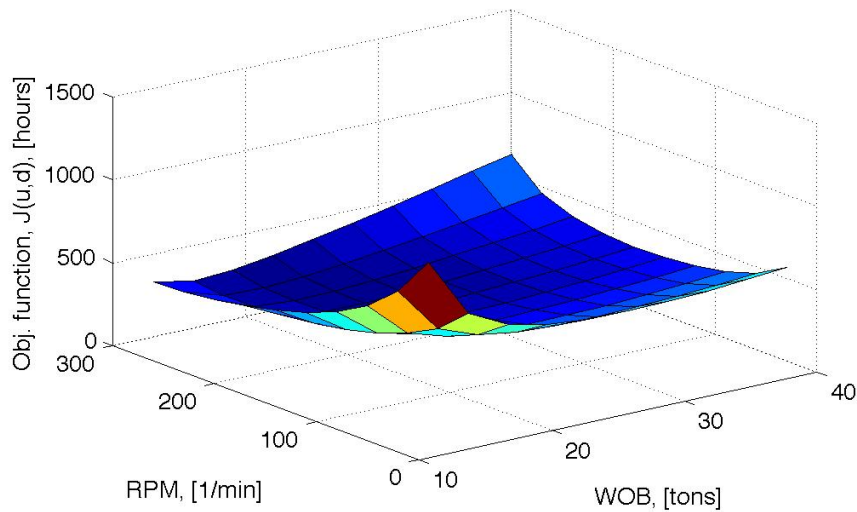


Figure 4.2: Surface plot of the objective function $J(u,d)$ versus the WOB and the drill string RPM.

The remaining task is to determine what variables should be controlled by the two unconstrained degrees of freedom in the drilling process. The choices of controlled variables may give very different results when the drilling process is subject to disturbances. This will be analyzed in Chapter 5.

Chapter 5

Self-Optimizing Controlled Variables

This section will cover the process of selecting the variables that should be controlled during the drilling process. The theory was described in detail in Section 2.3.

The results of Chapter 4 showed that two degrees of freedom must be used to control the active constraints. Assuming the MPD system with the choke and backpressure pump is used to control the bottomhole pressure and the mud circulation rate is kept at its constrained value, we are left with two manipulated variables:

- Weight on Bit (W)
- Drill string rotary speed (N)

The manipulated variables can be used to control various measurements in order to gain more profitable operation when the drilling process is subject to disturbances.

The best controlled variables may be identified by a *brute-force* evaluation, implementing control of various combinations of controlled variables, introducing the expected disturbances and calculating the loss compared to the re-optimized value of the objective function. While the process only involves two unconstrained degrees of freedom and thus two controlled variables left to determine, a brute-force evaluation is rather tedious work. We have six variables available after removing the bottom hole pressure, choke pressure and mud flow rate from the analysis. Therefore, we are left with $\frac{6!}{2!4!} = \binom{6}{2} = 15$ combinations of controlled variables. It is important to recognize that the manipulated variables are treated as measurements when determining the controlled variables. In case a manipulated variable is used as a controlled variable, it means that it is beneficial to keep the MV constant.

Instead of performing a brute-force evaluation, we may determine the self-optimizing controlled variables by various mathematical methods. The procedures and results of the maximum scaled gain (minimum singular value) method, the null space method and the exact local method are described in Sections 5.2, 5.3 and 5.4.

5.1 Process Gains and Disturbances

The process gains from the inputs to the measurements (outputs) can be achieved by applying small perturbations to the manipulated variables. The magnitude of the perturbations was 1% of the nominal value. The calculation is performed as shown in Equation 5.1, and the gain matrix is presented in Appendix B. The MATLAB script is presented in Appendix E. The inputs themselves are included as the bottom two measurements in the gain matrix, so the bottom 2×2 matrix is naturally an identity matrix.

$$G_{i,j} = \frac{\Delta y_i}{\Delta u_j} = \frac{y_i - y_i^0}{u_j - u_j^0} \quad (5.1)$$

The first steps in selecting the optimal controlled variables is identifying the sensitivity of the measurements to various disturbances. As described in Section 3.2.1, the parameters related to the formation strength were all modeled to be functions of the drillability parameter R_0 . In addition to the formation strength, disturbances in the formation density and the bottom hole pressure were introduced. The disturbance parameters were perturbed 1%, and the drilling process was re-optimized after each disturbance in order to determine the optimal variation of the process variables. The disturbance sensitivity matrix F was calculated using Equation 5.2, and is presented below. The left column of F represents the disturbance in formation drillability (R_0), the middle column represents the disturbance in formation density (ρ_s), while the rightmost column represents the disturbance in the bottom hole pressure (p_{bh}).

$$F_{i,j} = \frac{\Delta y_{i,opt}}{\Delta d_j} = \frac{y_{i,opt} - y_{i,opt}^0}{d_j - d_j^0} \quad (5.2)$$

$$F = \begin{bmatrix} 3.94 & 0.00 & -0.15 \\ -6.71 & -0.00 & -0.00 \\ -27.05 & 0.00 & 0.00 \\ 0.26 & 0.00 & -0.01 \\ -0.18 & -0.00 & -0.00 \\ 12.60 & 0.00 & 0.00 \end{bmatrix}$$

The expected magnitudes the disturbances are presented in Table 5.1.

Table 5.1: Expected Disturbances

Disturbance	Magnitude	Unit
R_0	-2.5	m/hr
ρ_s	500	kg/m^3
p_{bh}	10	bar

The expected implementation errors (n) for each measurement (y) were estimated based on assumptions of measurement sensitivity, and are presented in Table 5.2.

Table 5.2: Implementation Errors

Measurement (y)	Implementation error (n)	Unit
R	0.1	m/hr
T	3	kNm
P	30	kW
x_c	1.0	%
W	3	$tons$
N	10	min^{-1}

5.2 Maximum Scaled Gain (Minimum Singular Value) Method

The optimal variation of the measurements ($e_{opt} = \Delta y_{opt}$) when subject to the disturbances in Table 5.1 are calculated using Equation 5.3. Further, the optimal span of the measurements is calculated as shown in Equation 5.4. The results are presented in Table 5.3.

$$e_{opt} = \Delta y_{opt} = F W_d \quad (5.3)$$

$$span(z_i) = \max_d |e_{i,opt}| + n \quad (5.4)$$

Table 5.3: Optimal Variation, Implementation Errors and Expected Optimal Span

Measurement	e_{opt}	e_i	$span(z)$	Unit
R	9.85	0.1	9.95	m/hr
T	17.8	3.0	20.8	kNm
P	68	30	98	kW
x_c	0.6	1.0	1.6	%
W	0.5	3.0	3.5	$tons$
N	31	10	41	min^{-1}

The scaled gain matrix (G') is calculated by multiplying the output scaling matrix S_1 with the gain matrix G . As described in Section 2.3.2, the S_1 matrix consists of the inverse elements of the span along its diagonal. Combinations of 2×2 matrices are selected from G' , and the minimum singular value $\underline{\sigma}(G' J_{uu}^{-1/2})$ is calculated. The results are sorted by descending minimum singular value and presented in Table 5.4. The S_1 and G' matrices are presented in Appendix B.

The results indicate that the best controlled variables (CV's) during drilling are the topdrive power (P) and the weight on bit (W). The pairing of controlled and manipulated variables is fairly intuitive in this case. The weight on bit is kept constant while the rotational speed of the drill string is used to control the topdrive power at a constant set point.

Table 5.4: Minimum Singular Value Results

z_1	z_2	$\underline{\sigma}(G' J_{uu}^{-1/2})$
P	W	0.243
W	N	0.159
R	W	0.077
P	N	0.058
R	T	0.051
T	P	0.050
T	N	0.043
R	N	0.042
x_c	W	0.037
T	x_c	0.037
R	P	0.018
x_c	N	0.021
P	x_c	0.009
R	x_c	0.0000
T	W	0.0000

5.3 Null Space Method

We have two manipulated variables and three disturbances. However, we assume that the disturbance in drillability R_0 is the most prevalent and thus neglect the other disturbances. The assumption is supported by analyzing the disturbance sensitivity matrix F . The sensitivities to a disturbance in R_0 (the leftmost column) are much higher than the other disturbances.

Thus, we consider only one disturbance and choose $n_y = n_u + n_d = 2 + 1 = 3$ measurements to combine in order to calculate the optimal measurement combination using the null space method. It should not matter which measurements are selected. However, we analyze the disturbance sensitivity matrix F and pick measurements with smallest relative sensitivity. Thus, we choose to combine the measurements of the topdrive power (P), the weight on bit (W) and the drill string rotational speed (N).

The left null space of the new disturbance sensitivity matrix F (containing only the rows corresponding to P , W and N) was calculated, giving the measurement combination matrix ($H_{nullspace}$) below. The results were normalized so the Euclidean norm of each row in H was equal to unity.

$$H_{nullspace} = \begin{bmatrix} -0.01 & 1.00 & 0.00 \\ 0.42 & 0.00 & 0.91 \end{bmatrix}$$

The first row of $H_{nullspace}$ is approximately equal to controlling the weight on bit (W), while the second row indicates controlling a combination of the topdrive power (P) and the drill string RPM. Therefore, the results do not differ too much from those obtained using the method of maximizing the singular value. However, the nullspace method does not take implementation errors into account, and is therefore not the most reliable method for determining self-optimizing control variables.

5.4 Exact Local Method

We use the exact local method to determine the optimal measurement combinations for the controlled variables, this time considering the effects of implementation errors. The \tilde{F} matrix is constructed as shown below:

$$\tilde{F} = [F \ W_d \ W_n]$$

Using the exact local method, we may choose how many measurements we wish to combine in our controlled variables. The loss is reduced by increasing the number of measurements that are combined, but this also increases the complexity of the controller. In order to achieve the optimal measurement combination matrices H , we solve the optimization problem presented in Equation 5.5.

$$\min_H \|H\tilde{F}\|_2 \quad (5.5)$$

$$\text{subject to: } HG = J_{uu}^{1/2}$$

The exact local method was solved by vectorizing the appropriate matrices and solving a quadratic minimization problem subject to linear constraints. The procedures are shown in Appendix C. The optimal measurement combinations and the corresponding maximum losses are presented in Table 5.5. The complete tables with all the results of the exact local method are presented in Tables D.1 to D.5 in Appendix D. The rows of the measurement combination matrices H were normalized so the Euclidean norm of each row was equal to unity. The normalization should make it easier to interpret the effect of each individual measurement to the controlled variable.

The number of measurements that are combined the controlled variables declines as the table extends downward. The last row represents no control, thus keeping the inputs (WOB and drill string RPM) constant. When only two measurements are combined, the measurement combination matrix H is irrelevant and single measurements can be chosen instead. This can be seen from Equation 5.6. If H is a square matrix we get $HH^{-1} = I$, and it is clear that the choice of H has no effect on the loss.

$$L = \frac{1}{2} \|J_{uu}^{1/2}(HG)^{-1}H\tilde{F}\|_2^2 \quad (5.6)$$

The loss decreases as we increase the number of measurements that are combined. This is expected, as the effect of the optimal variation of each measurement is reduced by combining an increasing amount of measurements. A graphical representation of the losses plotted against the number of measurements is presented in Figure 5.1.

The losses in Table 5.5 are the maximum losses, in other words the loss when the magnitude of the expected disturbances (d') and implementation errors (n') is unity. Figure 5.2 shows a graphical representation of the loss function for the six candidate optimal measurement combinations (presented in Table 5.5) as a function of the magnitude of the disturbances and implementation errors. The results show that the loss using a constant input policy is less than six hours higher than the optimal combination of two measurements (P and W).

Figure 5.3 shows the maximum losses with some selected two-measurement combinations that give very high losses. Several of the combinations may sound like good variables to control, if the system is not analyzed properly. The figure is meant to illustrate the importance of choosing good controlled variables.

Table 5.5: Optimal Controlled Variables

Description	CV's (CV ₁ on top, CV ₂ on bottom)	Max. loss
6 measurements	$0.75 R + 0.40 T + 0.02 P + 0.001 x_c + 0.53 W - 0.07 N$ $-0.39 R - 0.11 T + 0.16 P - 0.001 x_c - 0.77 W + 0.46 N$	1.87
5 measurements	$0.75 R + 0.40 T + 0.02 P + 0.53 W - 0.07 N$ $-0.39 R - 0.11 T + 0.16 P - 0.77 W + 0.46 N$	1.87
4 measurements	$0.70 R + 0.52 T + 0.50 W - 0.01 N$ $-0.19 R + 0.76 T - 0.36 W + 0.50 N$	2.02
3 measurements	$0.83 R + 0.56 T - 0.05 N$ $-0.51 R + 0.64 T + 0.58 N$	3.15
Single measurements	W P	6.24
Constant Inputs	W N	11.44

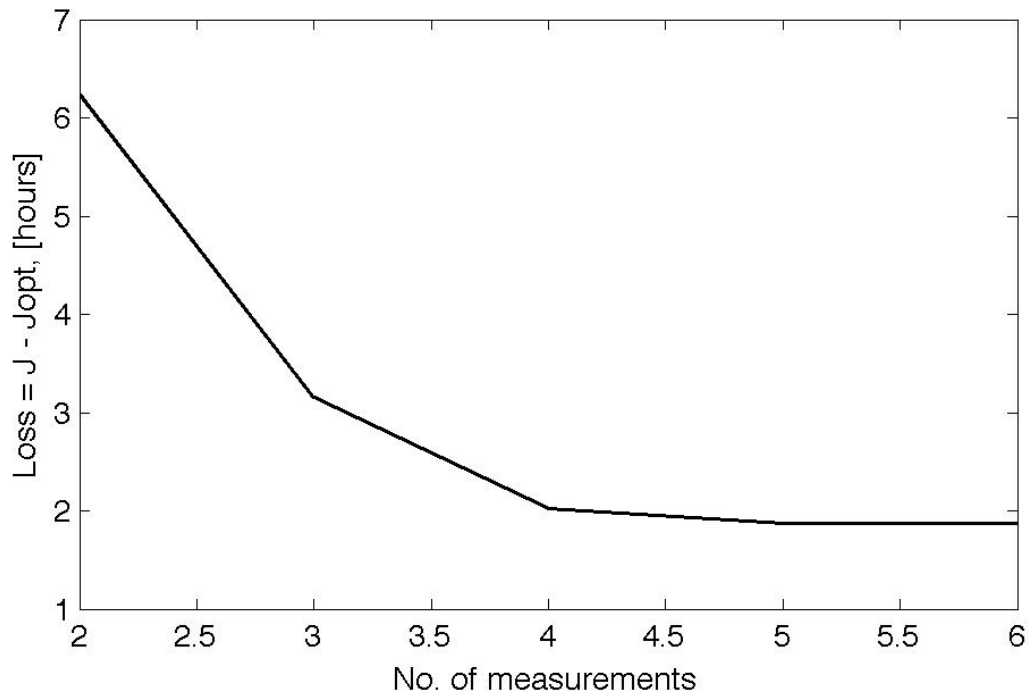


Figure 5.1: Plot of maximum loss versus the number of combined measurements.

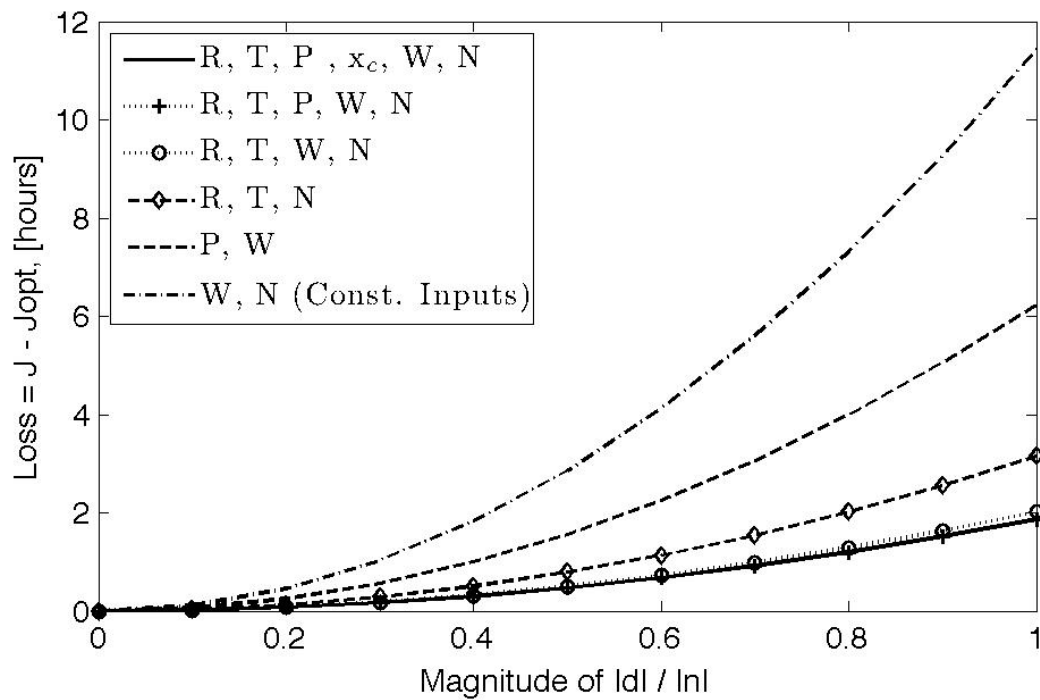


Figure 5.2: Plot of maximum loss of optimal measurement combinations versus the magnitude of disturbances.

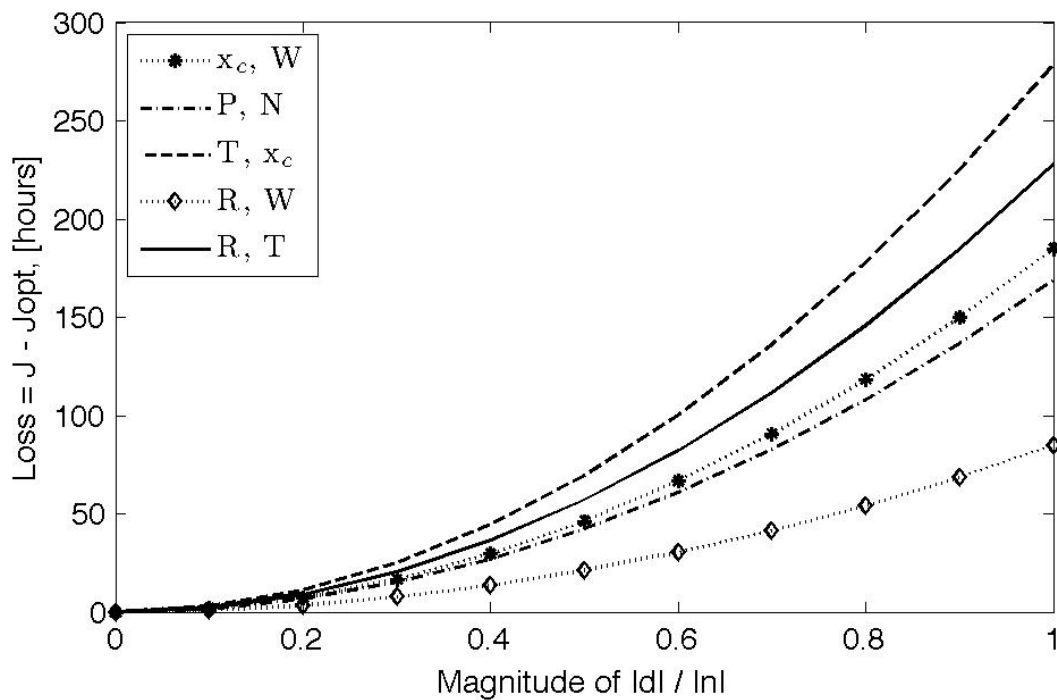


Figure 5.3: Plot of maximum loss of poor measurement combinations versus the magnitude of disturbances.

5.5 Pairing of Variables

The pairing of controlled variables with manipulated variables is usually determined by calculating the relative gain array (RGA), and choosing combinations that have a positive relative gain as close to one as possible.[5, 17] However, the pairing of variables is irrelevant when solving the exact local method with more measurements (y) than inputs (u), because the measurement combination matrix H will be multivariable itself.

Equation 5.5 on page 37 showed the optimization problem associated with the exact local method. The optimal solution H of the measurement combinations is non-unique.[11] From Equation 5.6 on page 37, we see that any non-singular matrix D of size $n_u \times n_u$ will be a solution to the exact local method. We introduce $H_1 = DH$, and apply it to Equation 5.6. The result of the loss variable is presented in Equation 5.7. D is invertible because it is a square, non-singular matrix.

$$J_{uu}^{1/2}(H_1G)^{-1}H_1\tilde{F} = J_{uu}^{1/2}DD^{-1}(HG)^{-1}H\tilde{F} = J_{uu}^{1/2}(HG)^{-1}H\tilde{F} \quad (5.7)$$

The result is that we have an extra degree of freedom in choosing the measurement combinations. We may, e.g. choose $D = (HG)^{-1}$ and get $H_1G = DHG = I$, thus resulting in a diagonal decoupling. As mentioned above, the consequence of this degree of freedom is that calculating the RGA and pairing variables is not relevant for measurement combinations. The pairing and H matrix may be chosen as desired by selecting the appropriate D matrix.

The pairing for the optimal single measurement controlled variables (two measurements), however, must be determined. In this case, it is fairly intuitive. The weight on bit (W) is kept constant, while the drill string RPM (N) is used to control the topdrive power (P). Interpreting this control structure physically tells us that as the formation strength increases, the power is kept at a constant set point by reducing the drill string RPM. Refer to Section 3.1 for the equations. This control structure will give less loss than keeping the inputs constant, as seen in Table 5.5 and Figure 5.2.

In addition to the self-optimizing controlled variables determined in this section, we chose to control the bottom hole pressure (p_{bh}) with the annulus choke pressure (p_c) and keep the mud circulation rate (the main mud pump flow rate, q_{in}) at a constant set point. This is because they represent active constraints at optimum, as explained in Section 4.5.

5.6 Discussion

The previous sections have determined the optimal single measurement controlled variables, and the optimal measurement combinations for combining three to six measurements. However, the question that yet remains is, how many measurements do we wish to combine? The loss is reduced by increasing the number of measurements that are combined in the controlled variables, as the effect of the optimal variation of each measurement is reduced. On the other hand, implementing measurement combinations complicates the control structure which naturally is undesirable. We wish to keep the control structure as simple as possible in order to facilitate easier understanding

of the controllers and also ease the tuning.

The graphical representation of the loss versus the number of measurements in Figure 5.1 shows us that the reduction in loss from combining more than four measurements is negligible. Thus, we should not worry about using more than four measurements in the controlled variables. The next question is whether we want to choose single measurements for the controlled variables, or whether we want the lower loss, but increased complexity, of introducing measurement combinations. In the case of measurement combinations being chosen, one might as well combine four measurements instead of three. The difference in controller design is minimal, but the reduction in loss is more prominent (see Figure 5.1).

The last option available is not selecting any controlled variables for the two unconstrained degrees of freedom, thus keeping them at constant values. The expected loss with such a constant input policy was shown in Figure 5.2. The loss is less than 12 hours of a total *active* drilling time of approximately 550 hours. The time spent making pipe connections and drilling trips, as well as the non-productive time is not included in the active drilling time. Thus, the loss with constant inputs is 2.2% of the active drilling time. The loss when controlling the optimal combination of four measurements is 2 hours. This means that the savings with a measurement combination control structure are approximately 10 hours, or 1.8% of the active drilling time. Similar results have been reported in drilling literature by Reed [18] and Galle and Woods [19]. Reed [18] indicated a difference of less than 3% between constant and variable bit weight and rotary speed for the cases studied, while Galle and Woods [19] reported that the costs were only slightly higher with constant inputs.

The optimal controlled variables using single measurements are the topdrive power and the weight on bit. This control structure gives a loss of approximately 6 hours. Thus, the savings compared to a constant input policy are less than 6 hours, or 1.1% of the active drilling time.

The drilling process is subject to much uncertainty regarding unforeseen events and accidents such as stuck pipe, drilling kicks and equipment failure. These incidents necessitate non-productive time on the drill rig, which is just as costly as the time spent drilling. According to Godhavn [20], the non-productive time may count up to 30% of the total drilling time. Compared to non-productive times of such magnitudes, savings of 1-2% in active drilling time seem negligible. However, the per-day rate of drilling is very costly, and any time saved equals a substantial revenue.

Another possibility is to discard the constant set point policy and control of self-optimizing controlled variables, and rather install a real-time optimizer (RTO). Eren and Ozbayoglu [21] suggest that real-time optimizers will be widely used in future drilling activities. A RTO is hierarchically positioned above the control layer (see Figure 2.2 on page 10), and continuously optimizes the drilling process for the process parameters at the given time. The RTO unit then passes the optimal values of the process variables as set points to the control layer, as illustrated in Figure 2.4 on page 13. However, installing a RTO requires an on-line computer database with a continuous feed of accurate drilling parameters. Real-time optimization may not be as reliable as operating with constant set points, and may prove to involve more effort than is reflected in the outcome. The loss with a constant set point policy for a optimal combination of measurements very small relative to the total drilling time. It may be likely that the increased savings of installing an RTO are not worth the increased complexity of the control structure.

5.7 Stick-Slip Phenomenon

The drill string is a long, relatively thin-walled metal pipe extending several thousand meters. It is natural that the drill string experiences vibrations during drilling. The vibrations are classified as torsional, axial and lateral vibrations, each presenting a challenge to the drilling process. Torsional vibrations may result in *stick-slip* oscillations of the drill string, while axial vibrations may cause the drill string to oscillate along its vertical axis, thus making the bit *bounce* against the bottom of the well. Lateral vibrations may cause the drill bit to rotate around multiple centers in the borehole in a *whirling* fashion, thus drilling an oversized hole and reducing the rate of penetration. The *stick-slip* phenomenon is in particular considered to be a major problem in drilling operations, and has been frequently addressed in drilling literature.

Torsional vibrations in the drill string and the stick-slip phenomenon arise from the difference between static and dynamic friction. Various downhole conditions such as drag, doglegs (bends), tight hole sections or formation characteristics may cause the bit to temporarily get stuck or *stall* in the formation while the topdrive continues to rotate the drill string. The result is that torsional energy is built up in the drill string until the energy overcomes the static friction between the drill bit and the formation. Since the dynamic friction is lower than the static friction, the drill string has excessive energy stored up to propel itself around. The result is that once the bit comes loose, it rotates or *whips* around at a very high speed. This creates a torsional wave that travels up the drill string to the surface and the topdrive. If the topdrive is operated at a constant speed, it will act as a fixed end to the drill string and reflect the torsional wave back down. When reaching the bit, the torsional wave may cause it to stall again, thus repeating the stick-slip cycle. The stick-slip motion causes fatigue to the drill string, specially at the pipe connection joints, and causes severe axial and lateral vibrations during the *slip* phase. The consequences are excessive bit wear and a reduced rate of penetration.[22, 23]

The stick-slip phenomenon can be encountered even without the effect of physical conditions such as described above. At low rotational speeds, the transition between static and dynamic friction causes a drop in the frictional torque, as shown in Figure 5.4.[22, 24, 25] The negative slope of the friction torque with respect to the rotational speed has an anti-damping effect, causing the magnitude of the stick-slip phenomenon to increase with each cycle. Thus, when operating with a drill string rotational speed in the transition phase, the drill string will experience self-sustained stick-slip oscillations. Increasing the rotational speed above the *critical* speed will cause the oscillations to be dampened and thus eventually reach a constant value. However, the optimal rotary speed may be lower than the critical speed for torsional oscillations. Therefore, it is desirable to be able to operate in this region without experiencing the stick-slip phenomenon.

Several solutions to eliminate stick-slip have been presented in drilling literature, such as soft-torque systems, manipulating the weight on bit (WOB) or introducing a vibration damper in the bottom hole assembly (BHA).[22] The solution involving the use a torque feedback control system with a varying drill string rotational speed seems to be most widespread.[26, 27] In conventional drilling, the topdrive is designed to keep the rotational speed of the drill string at a constant value. As described above, such a system will reflect the torsional wave and introduce stick-slip oscillations if operated below the critical RPM. Instead, Halsey et. al. [26] proposed letting the topdrive respond to the dynamic torque oscillations in such a way that the vibrations are dampened or absorbed. The control system involved implementing torque measurement at the drilling floor and controlling the torque by manipulating the rotational speed of the drill string.

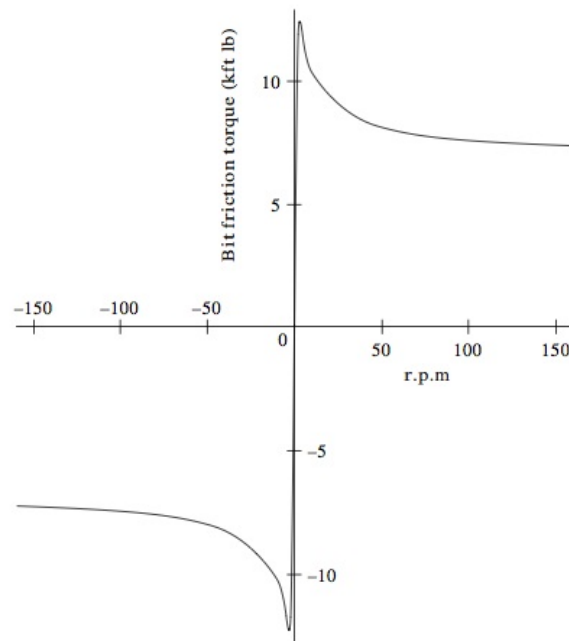


Figure 5.4: Plot of friction torque as a function of rotational speed of the drill string.[25]

The torque feedback control system was studied further by Javanmardi et. al. [27], implementing a direct measurement of the torque from the topdrive motor current and voltage measurements. The system was tested on off-shore wells with significant reductions on torque fluctuations and stick-slip conditions. In addition, the performance of the torque feedback control system was found to increase when reducing the inertia of the topdrive.[28]

The problems regarding the stick-slip phenomenon seem to be closely related to keeping a constant drill string rotational speed. Applying the results from the drilling literature that were described above, we may assume that a constant input (WOB and drill string RPM) control structure could potentially be subject to stick-slip conditions and thus give non-optimal drilling operation. On the other hand, using the drill string rotational speed to control the topdrive power, or other combinations of measurements, implies a varying rotary speed input. Disturbances in lithology that may provoke stick-slip will be compensated by the rotational speed of the drill string in order to keep the controlled variable at its set point. Thus, it is likely that varying the drill string RPM will reduce the reflection of torsional vibrations from the topdrive and thus dampen stick-slip oscillations in a similar manner as the torque feedback systems of Halsey et. al. [26] and Javanmardi et. al. [27].

Other solutions to avoid stick-slip conditions involve increasing the rotational speed above the critical value. However, an excessive drill string RPM may lead to lateral vibrations, that again reduce the rate of penetration.[22] Additionally, merely changing an input from its optimal value will result in non-optimal operating conditions. The increase in drill string RPM may however be compensated (or even completely substituted) by reducing the weight on bit, since the torque is dependent on the WOB. The structure of such a control system is quite sophisticated. Therefore, an alternative solution to avoiding stick-slip could be implemented in a supervisory control layer (refer to Figure 2.2 on page 10), involving a model predictive controller (MPC). Recognizing stick-slip conditions, the MPC could optimize the process (avoiding stick-slip) and determine new optimal set points for the weight on bit and drill string rotational speed.

Chapter 6

Pressure Control and Automation

Although it is important to drill fast and efficiently, the efficiency during non-drilling operations such as pipe connections and trips is equally important to optimize the total drilling process. These operations make up a significant portion of the total time, as explained in Section 4.2.

During the entire drilling process, it is important to accurately control the pressure profile of the well in order to prevent unwanted influx of reservoir fluids or outflux (loss) of mud into the formation. This is a challenging task, as the procedures during pipe connections and drilling trips have a large impact on the pressure. Since the main pump is disconnected for each connection, the mud circulation is stopped and the pressure term due to friction is lost (refer to Section 3.1). Similarly, full retraction of the drill string (trip) increases the volume of the well and lowers the height of the mud column, leading to a loss of hydrostatic pressure. Using MPD technology, these disturbances can be compensated for using the choke valve and back pressure pump to control the bottom hole pressure as explained in Section 2.1.1.

The performance of the pressure control system is essential to the speed of these operations. Referring to Equation 4.6 on page 27, minimizing t_c^0 and t_t^0 will minimize the total drilling time and costs. However, it is important to realize that these operations are independent from the actual drilling tasks. During connections and trips, pressure control and the speed of operations are the only relevant control objectives.

During a pipe connection or trip, the task of ramping down the main pump while simultaneously ramping up the back pressure pump and keeping the bottom hole pressure within its margins is a challenging task for the drillers. It would be highly beneficial to design an automated procedure and control system for each pipe connection process, as well as trips. Ideally, the operator would only need to initiate e.g. a *pipe connection program* and the required procedures would be handled automatically by the drilling control system.

6.1 Pressure Control Structure

The drilling model that was described in Chapter 3 and used in Chapters 4 and 5 used the choke pressure (p_c) as a degree of freedom. It was assumed that the choke pressure is manipulated in order to control the bottom-hole pressure, as part of the managed pressure drilling (MPD) system. This section will study the performance of the MPD system, in terms of how the pressure control structure may be designed.

As described in Section 2.1.1, the top of the annulus is sealed off by a rotating control device (RCD) so that the flow of mud may be controlled by a choke valve. A back pressure pump is also connected to the annulus, so pressures which are in excess of the capacity of the valve may be achieved. A schematic is presented in Figure 6.1, showing an overview of the well. The left side shows the equipment and connections to the drill string, while the right side focuses on the well annulus.

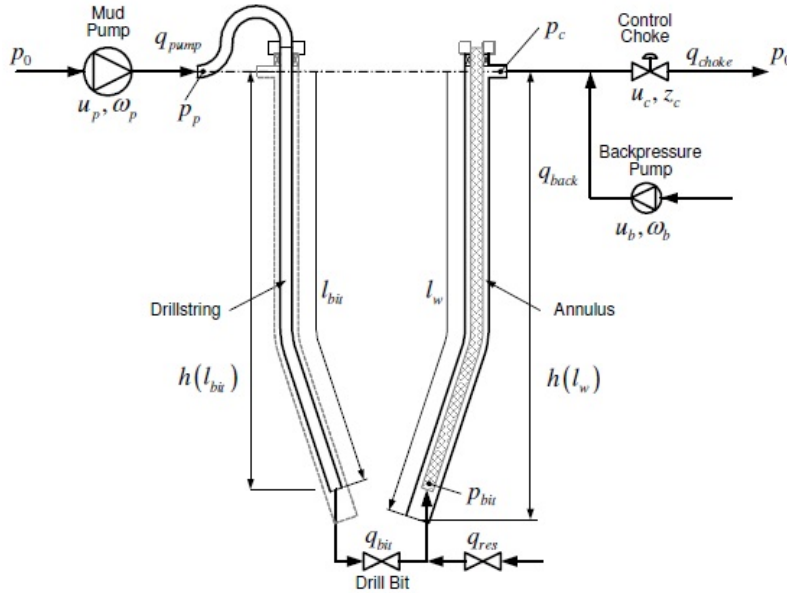


Figure 6.1: Schematic of a well, with drilling mud circulation system.[2, 29]

Since the bottom hole pressure is dependent on the annulus mud flow, it is possible to use the main mud pump flow to control the pressure. However, in Section 4.5 we determined it to be optimal to control the main pump flow rate at its upper constraint of 50 liter/s. Anyhow, the main pump can not be used for pressure control during pipe connections since it must be disconnected from the drill string. Therefore, it is beneficial to find other variables for control. A cascaded control structure with input resetting has been proposed for controlling the bottom-hole pressure. A block diagram of the control structure is presented in Figure 6.2.

The bottom hole pressure is controlled by a cascade controller (K_1 in Figure 6.2) which uses the choke pressure set point ($p_{c,s}$) as an input. The choke pressure (p_c) is controlled using the choke valve opening (controller K_2 in Figure 6.2). However, the valve may not have the sufficient range for control. In this case, the back pressure pump may be used to elevate the choke pressure. We may view this type of co-ordination of inputs as an input resetting control structure. Little or no

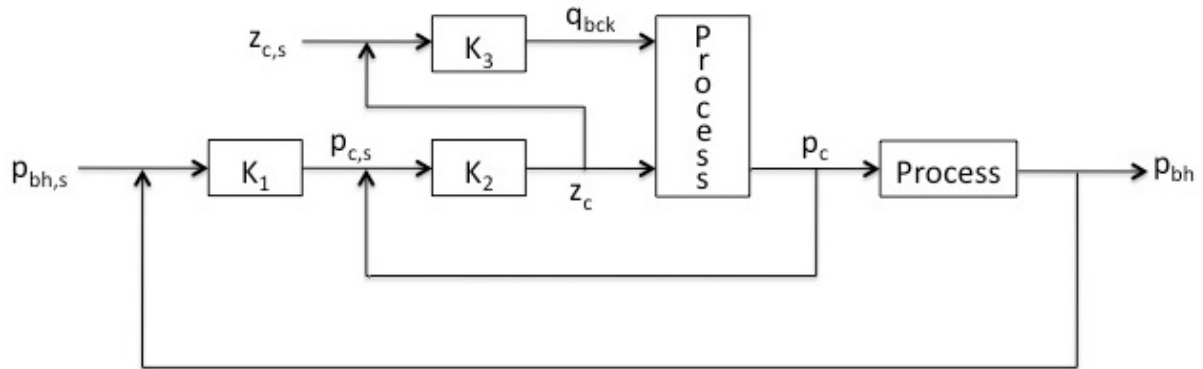


Figure 6.2: Block diagram of the pressure control structure.

action is needed by the back pressure pump as long as the choke valve position is close to 50%, as the valve should be able to operate in a certain range. However, the valve position may change very quickly during pipe connections and trips, thus making a *slow loop* input reset controller inappropriate in this case. The issue was solved by raising the valve position controller error to the third power, making the input reset controller (K_3 in Figure 6.2) a non-linear controller. The result is high controller action when the valve position is far from its set point of 50%, but little action when the valve position is in an acceptable range.

6.2 Pipe Connections and Drilling Trips

In order to optimize the drilling process, we wish to minimize the pipe connection time t_c^0 and the trip time t_t^0 . In order to simulate the effect on a pipe connection or a trip on the drilling process, we first need to identify the procedures which take place. During a pipe connection, the topdrive and mud pump must be disconnected from the drill string in order to facilitate the connection. While the main pump is ramped down, the drillers must be able to rely on the pressure control system to keep the bottom-hole pressure at its set point (minimum between its margins). Thus, a pipe connection involves the following sequence of procedures: [30]

1. Position drill string to roughneck position
2. Stop drill string rotation
3. Engage slips
4. Ramp down main mud pump
5. Perform physical connection
6. Ramp up main mud pump
7. Release slips
8. Start drill string rotation
9. Trip in drill string to bottom of the well

A drill trip involves a full retraction of the drill string from the well. Thus, it may be viewed as a series of retracting the length of one stand of pipe and performing a reversed connection procedure.

The speed of pipe connection and tripping operations is naturally dependent on certain procedures that must be assumed to require a constant amount of time, such as the physical connection procedure. The speed of other procedures, however, such as ramping the main pump up/down and tripping the drill string in/out may possibly be improved. Changing the mud circulation rate or the drill string position will affect the bottom hole pressure. Therefore, it is important that these procedures are performed quickly (to minimize the cost), but without causing excessive upset to the bottom hole pressure. The possible consequences of poor pressure control were addressed in Section 2.1.

In order to facilitate optimal operation of drilling trips and pipe connections, it is important that the mud flow rate and drill string velocity is automatically controlled rather than manually controlled by the drillers. It would be optimal to configure automated sequences for pipe connections and trips that could easily be initialized by the operators.

6.2.1 Automation with Controllers

We want to implement control of the mud circulation rate and the depth of the drill string, so the operators will only need to change the set point of the corresponding variable to its desired value. This can be done by implementing controllers for the main mud pump flow rate and the vertical position of the drill bit. However, the controller responses must be slow enough to maintain the bottom hole pressure within its margins. To achieve this type of response, we include *switches* in the control structure. The MATLAB Simulink switch block is shown in Figure 6.3.

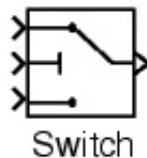


Figure 6.3: MATLAB Simulink switch block.

The switch block accepts three inputs, and the output is selected as either the first or third input based on the value of the second input. In this case, the first input involves no action at all, while the third input is the proposed action by the controller. The second input is chosen as the absolute difference between the bottom hole pressure and its set point. If the absolute error is greater than the passing criteria of the switch, no action is applied to the corresponding variables. On the other hand, if the pressure is within the boundaries of the passing criteria, the PI-controller action is applied. A block diagram of the complete pressure control structure with the addition of controllers for the main mud pump flow rate and the position of the drill bit is presented in Figure 6.4. When initializing a pipe connection sequence, the operator simply changes the main mud pump flow rate set point to zero. The controller will reduce the pump flow rate as fast as possible while maintaining the bottom hole pressure within the margins defined by the passing criteria of the switch. When ramping up the pump, the desired flow rate is applied as the new set point and the controller takes care of the dynamics. The same applies for a drilling

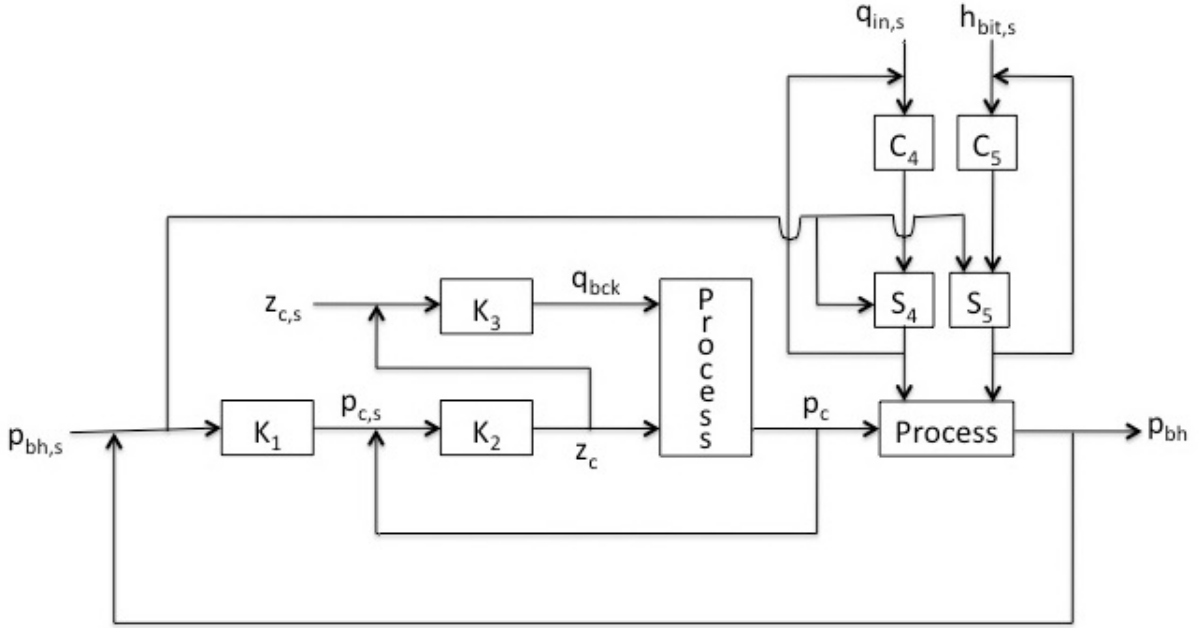


Figure 6.4: Block diagram of the pressure control structure with controllers for the main mud pump flow rate and drill bit position.

trip. The operators apply a new set point for the position of the drill bit corresponding to the length of one stand of pipe, and the controller performs the tripping in/out as fast as possible with respect to the bottom hole pressure.

6.3 Dynamic Pressure Model

A simple dynamic pressure model in MATLAB was used to test the performance of the pressure control structure. The model was based on the work of Kaasa [29], and the assumptions of one-dimensional flow with constant density in an annulus with constant cross-sectional area. The equations are derived from the continuity- and momentum equation(s) and are presented in presented in the work of Stamnes [2, 31]. The differential equations of the model are presented in Equations 6.1 through 6.3.

$$\frac{V_a}{\beta_a} \dot{p}_c = q_{bit} - q_c + q_{bck} \quad (6.1)$$

$$\frac{V_d}{\beta_d} \dot{p}_p = q_p - q_{bit} \quad (6.2)$$

$$M \dot{q}_{bit} = p_p - p_c - \theta_1 q_{bit} - \theta_2 |q_{bit}| q_{bit} \quad (6.3)$$

The bottom hole pressure is calculated from Equation 6.4, and the choke pressure is calculated from the choke equation presented in Equation 6.5.

$$p_{bh} = p_c + \theta_1 q_{bit} + \rho g D \quad (6.4)$$

$$q_c = K_c z_c \sqrt{\frac{2}{\rho_m} (p_c - p_0)} \quad (6.5)$$

Linear friction is assumed for the well annulus while quadratic friction is assumed for the drill string. Similar to Equation 3.25 on page 22, the pressure drop due to friction was modeled with friction parameters θ_1 and θ_2 . The pressures p_p and p_c are in units *barg* and represent the main pump pressure and the choke pressure, respectively. p_0 represents the atmospheric pressure, and since the units are *barg* we have $p_0 = 0$. The flow rates q_p , q_{bck} , q_{bit} and q_c represent the rates of the main pump, the back pressure pump, the flow rate through the bit and the flow rate through the choke valve. K_c is the valve constant, and has units m^2 . V_a represents the volume of the well annulus, and is calculated from the same parameters that are presented in Table 3.2. V_d represents the internal volume of the drill string, and is calculated using the inner diameter specification in Table 6.1. β represents the bulk modulus of the drilling mud, and is a measure of the mud's resistance to compressibility. The parameter M is the sum of the mass coefficients M_a and M_d , which are defined in Equations 6.6 and 6.7.

$$M_a = \frac{\rho D}{A_a} \quad (6.6)$$

$$M_d = \frac{\rho D}{A_d} \quad (6.7)$$

The mud density is the same in the drill string as in the annulus, as the model is based on stationary conditions with zero rate of penetration. The returning mud is therefore not affected by cuttings that increase the effective mud density, such as in Equation 3.22 on page 21.

The model parameters are summarized and the values are presented in Table 6.1. The MATLAB scripts and functions for the simple dynamic pressure model are attached in Appendix E.

Table 6.1: Dynamic Pressure Model Parameters

Parameter	Description	Value	Unit
d_b	Drill bit diameter	0.254	m
d_s	Drill string outer diameter	0.10	m
d_i	Drill string inner	0.085	m
V_a	Annulus volume	128.45	m^3
V_d	Drill string internal volume	17.02	m^3
β	Bulk modulus	20 000	bar
θ_1	Annulus friction parameter	900	$kg/m^4 s$
θ_2	Drill string friction parameter	180 000	kg/m^7
M	Mass coefficient	8 384	$10^5 kg/m^4$
D	Depth of well	3 000	m
ρ	Drilling mud density	0.0140	$10^5 kg/m^3$
K_c	Valve flow constant	0.0025	m^2

6.4 Simulations

6.4.1 Controller Design

The control structure presented in Figure 6.4 was implemented in the pressure model with PI-controllers for $K_1 - K_5$. The input reset controller (K_3 in Figure 6.4) was modeled as a non-linear controller, raising the choke valve position error to the third power. The controllers were manually tuned to give satisfactory control performance. Refer to Equation 2.30 on page 15 for the PI controller design equation, and to Seborg et. al. [17], Skogestad and Postlethwaite [5] or other process control literature for more information on the topic.

The switches (S_4 and S_5 in Figure 6.4) were designed to pass no action to their respective variables (the mud pump flow rate and the drill bit position) for bottom hole pressure errors greater than or equal to 5 bar in magnitude. For absolute errors of less than 5 bar, the normal PI action from the corresponding controller (K_4 or K_5) was passed. In other words, the bottom hole pressure is controlled within a pressure window of ± 5 bar.

6.4.2 Results

Figures 6.5 through 6.10 present the responses of the various process variables to the main procedures during pipe connection and/or drilling trips. The following takes place in the simulation:

- At time = 100 seconds, the set point for the main mud pump flow rate is set to zero.
- At time = 200 seconds, the set point for the drill bit position is increased by 27 meters, representing one stand of pipe.
- At time = 300 seconds, the drill bit position set point is set back to its original value of -3000 meters.
- At time = 400 seconds, the mud pump flow rate set point is set back to 3000 liter/min (50 liter/s).

The responses show that the pressure control structure is able to handle the disturbances in pressure that are caused by changing the main mud pump flow rate as well as the retraction and re-insertion of drill string. The ramping up/down of the main mud pump is performed as quickly as possible within the bottom hole pressure boundaries. Figure 6.8 shows that the pump is ramped down completely in approximately 50 seconds. Likewise, tripping one stand of drill pipe in/out is performed in approximately 10 seconds. This corresponds to a speed of approximately 3 m/s, which may be close to the physical limitations of the drawworks.

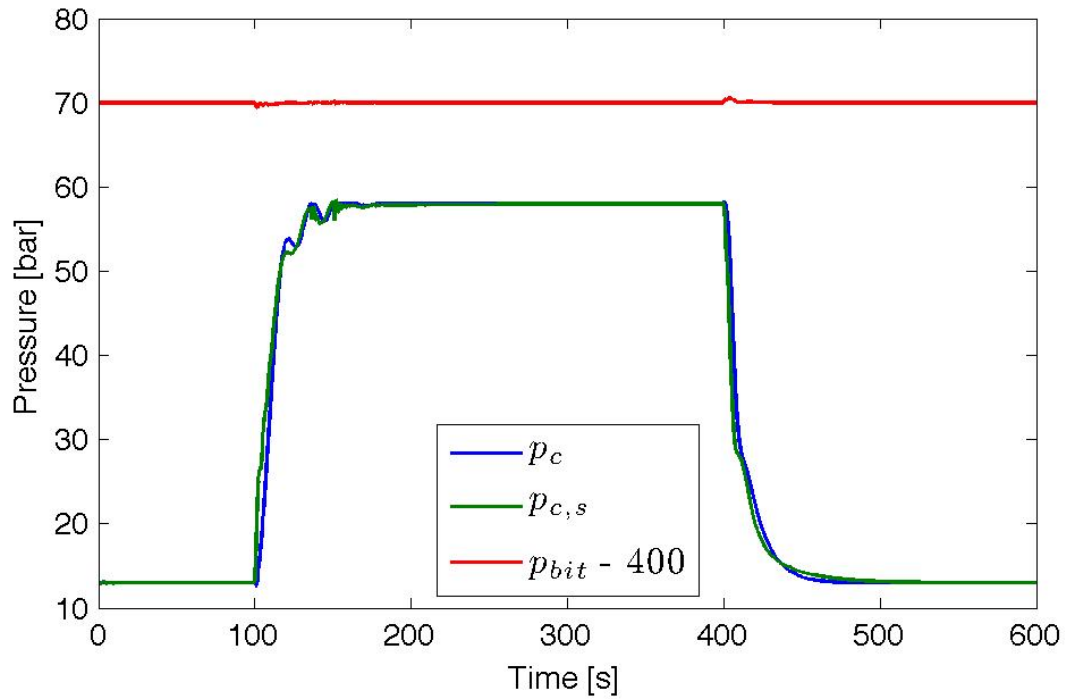


Figure 6.5: Bottom hole pressure, main pump pressure, choke pressure and choke pressure set point responses to a drilling trip simulation.

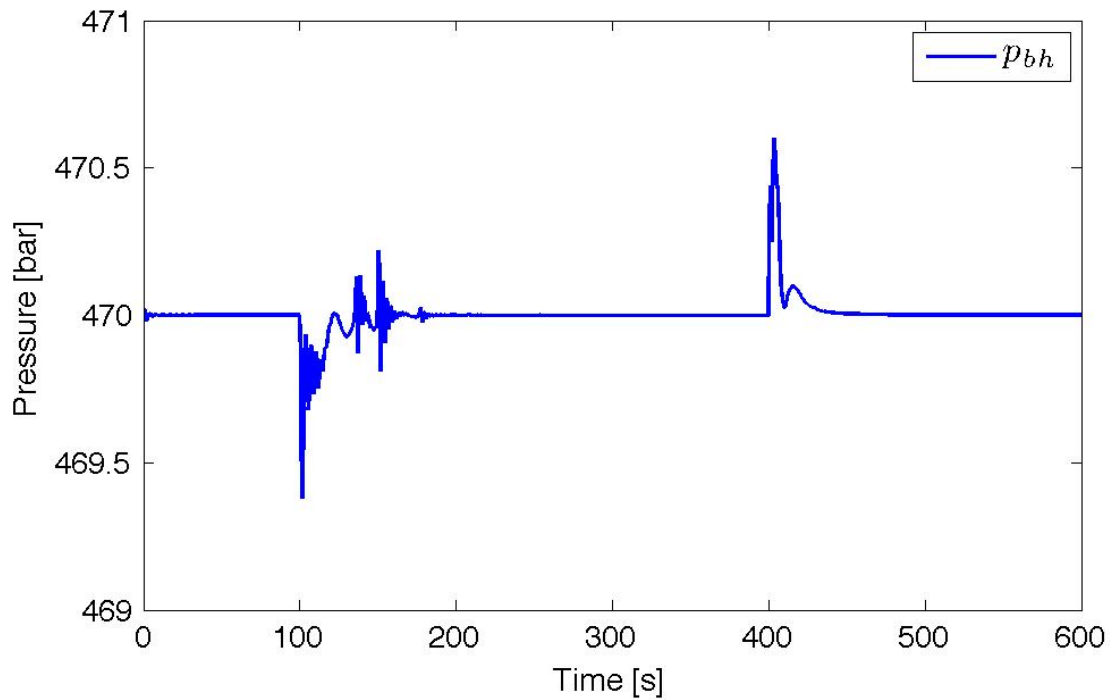


Figure 6.6: Close-up of the bottom hole pressure response in Figure 6.5.

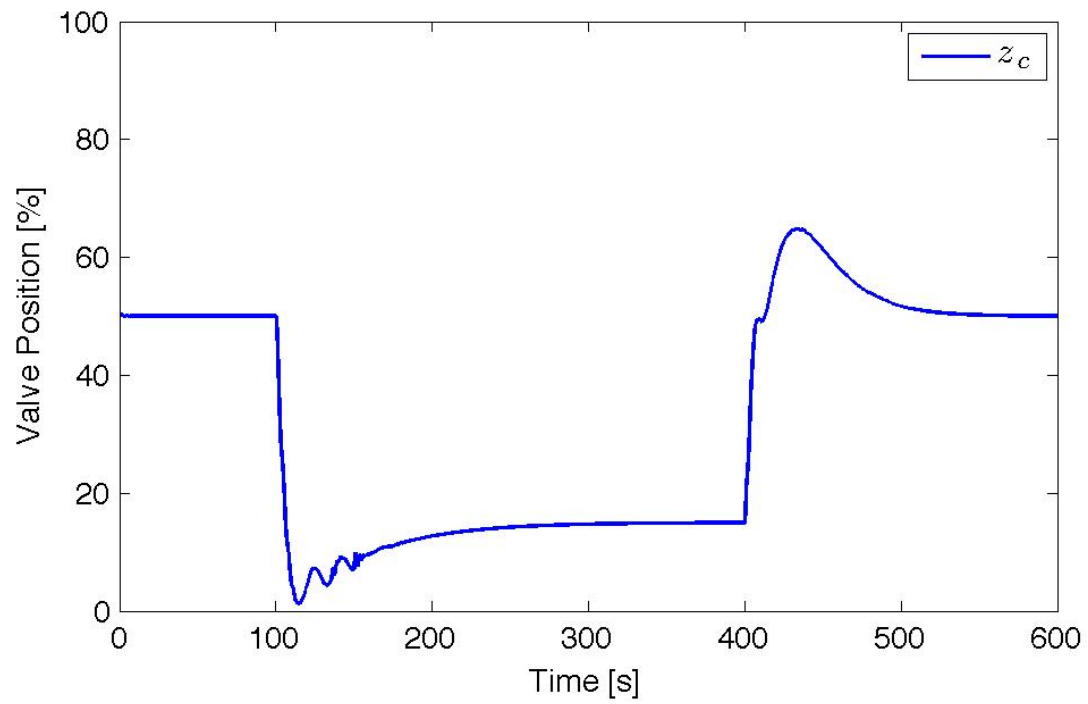


Figure 6.7: Valve position response to a drilling trip simulation.

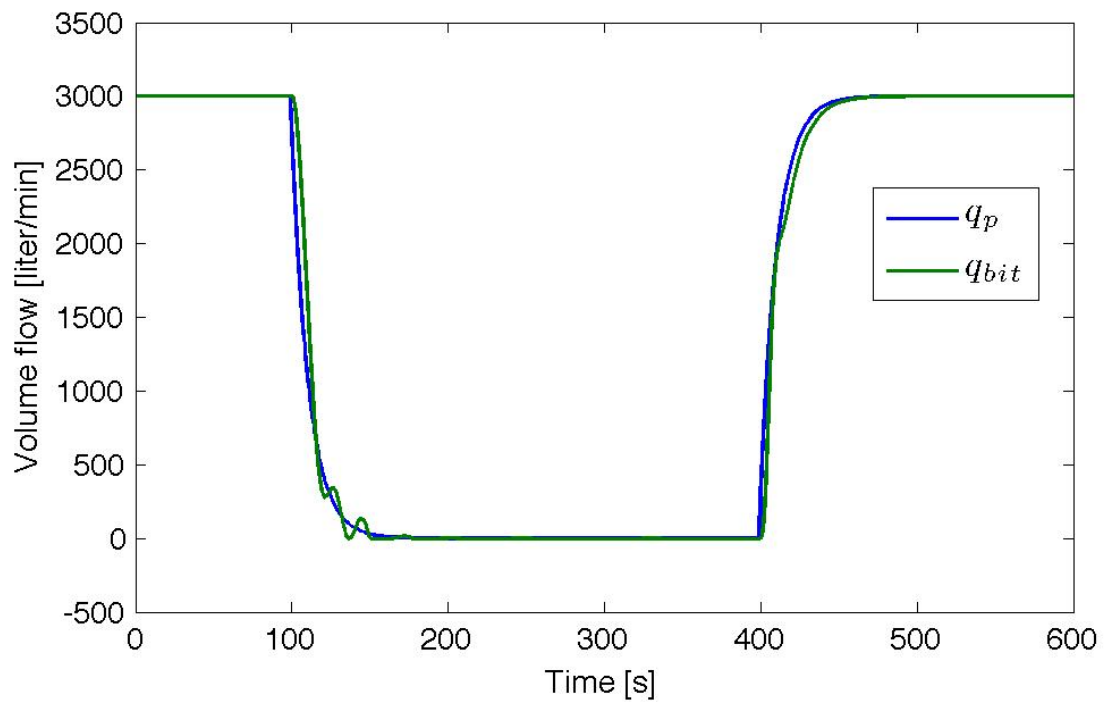


Figure 6.8: Main pump and drill bit flow rate response to a drilling trip simulation.

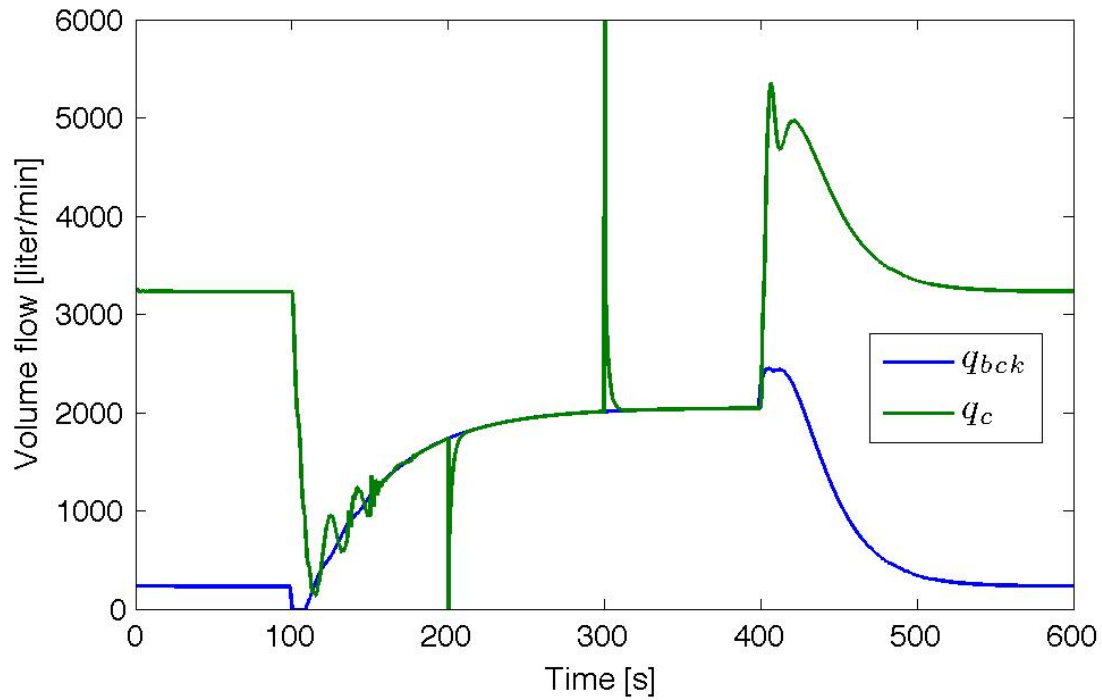


Figure 6.9: Back pressure pump flow rate and choke flow response to a drilling trip simulation.

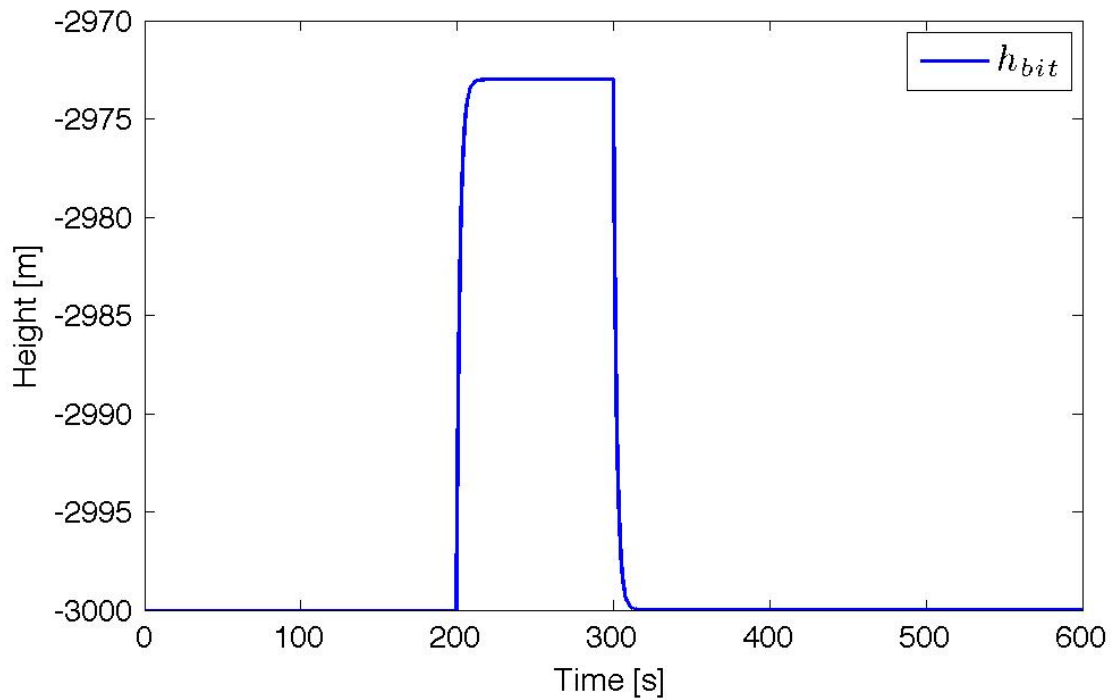


Figure 6.10: Drill bit vertical position response to a drilling trip simulation.

6.5 Discussion: Model Predictive Control (MPC)

The results in the preceding section show how simple PI controllers in the regulatory control layer may control the bottom hole pressure (BHP) while pipe connection and drilling trip procedures are performed. Alternatively, the control may be lifted to a supervisory layer (refer to Figure 2.2 on page 10) involving a model predictive controller (MPC) controlling the bottom hole pressure. A model predictive controller uses a linear algebra method for predicting the future responses to changing the manipulated variables. Once the model has been created the controller can use the model, in combination with current process measurements, in order to achieve the desired response by changing the appropriate manipulated variables accordingly.[32]

Breyholtz et. al. [33] demonstrated the use of control hierarchy (Skogestad [6]) to the Managed Pressure Drilling (MPD) system, with a MPC controller in the *supervisory* layer. The control structure is illustrated in Figure 6.11.

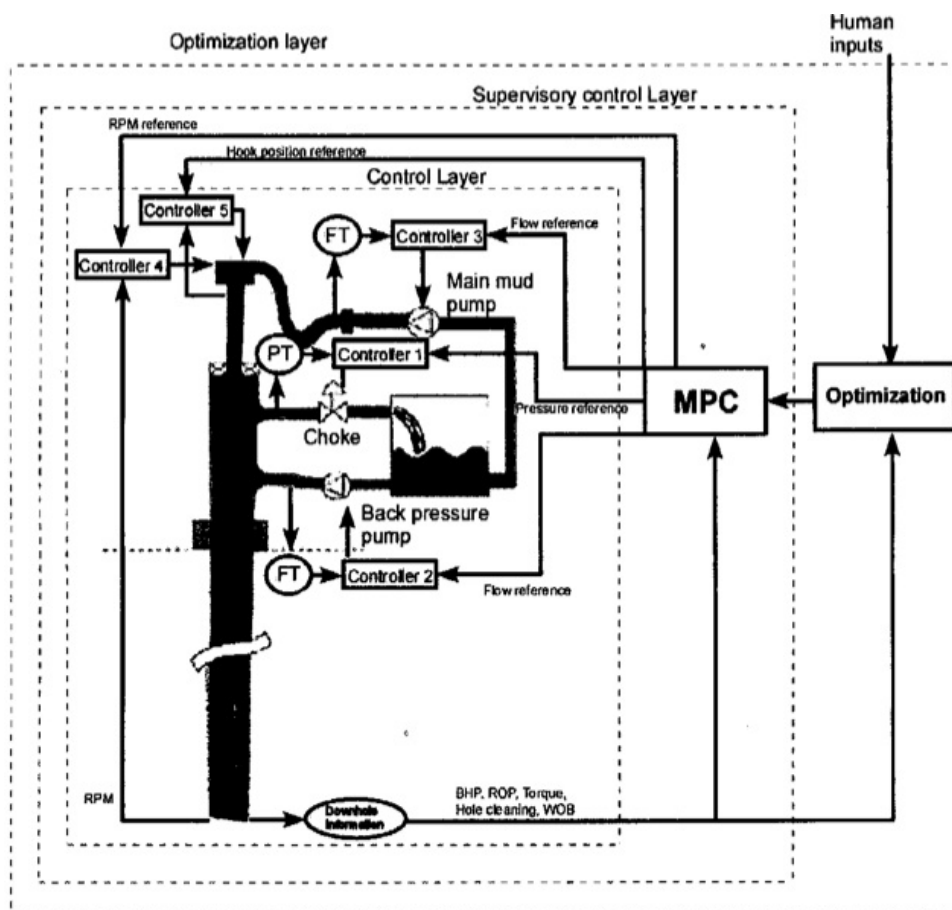


Figure 6.11: Illustration of the MPD well control system with control hierarchy.[33]

The regulatory control layer consists of feedback control loops with PID controllers (refer to Equation 2.30 on page 15). PID controllers are by far the most widely used control technology in the industry, mostly due to their simplicity and ease of tuning. The PID controllers accept set points from the MPC, and vary the corresponding manipulated variables accordingly.

One of the great advantages with model predictive controllers is the possibility of including

constraints to the controller. Thus, if the choke valve (z_c) reaches its constraints, the MPC controller can automatically compensate by providing a higher set point to the back pressure pump (q_{bck}) controller. Similarly, the main mud pump flow rate may be used to control the pressure profile during drilling operation, but is shut down by the MPC prior to pipe connections or drilling trip procedures. The MPC controller will accept operator inputs for the hook position (bit position) and main mud pump set points when applicable, and manipulate the process variable in order to reach the new set points while simultaneously controlling the bottom hole pressure.

The MPC controller could probably handle all the control tasks by itself, but the modeling effort is greatly reduced by the PID controllers in the regulatory layer. The model dependency is in fact one of the major disadvantages with model predictive controllers, as an accurate model is necessary to obtain good results. When working properly, a MPC will outperform the alternative strategy of a feedback control structure. However, the MPC performance is dependent on many parameters being correctly formulated, such as the model itself, the prediction horizon, control horizon, manipulated input weighting and sample time. Therefore, a feedback control structure consisting of PI controllers was presented in this thesis work as a feasible alternative.

Chapter 7

Conclusions and Further Work

7.1 Conclusions

The thesis work has involved an extensive search for- and review of drilling literature, in order to learn the process and the challenges that are faced during drilling operations. A steady-state model of the drilling process was modeled based on equations found in literature. Most of the drilling equations used are empirical and require parameter estimation for a large number of parameters. These estimates were made based on reported values in drilling literature, as well as trial-and-error procedures to re-produce realistic drilling results from the model.

The objective function, or cost function, of the drilling process was determined based on drilling literature, reasoning and analysis. The cost function was to reflect all parts of the drilling process, not only the active drilling time. Analysis of the objective function led to the separation of the drilling operations into two operating modes: *Active drilling* operations, and *pipe connections and drilling trips*. The reason for separating the process into two operating modes was the difference in control objectives. Thus, the optimization of the active drilling operations and the pipe connections and trips were analyzed separately.

7.1.1 Optimal Controlled Variables

The drilling process was optimized for given parameters representing the drilling conditions. The constraints on the bottom hole pressure and mud circulation rate were active at the optimum. It is optimal to control active constraints, so two degrees of freedom were removed from further analysis. The bottom hole pressure was controlled by the choke pressure, while the main mud pump flow rate was kept constant.

The expected disturbances were applied and the unconstrained drilling process was re-optimized in order to determine the optimal self-optimizing controlled variables. The results showed that there is negligible gain in combining more than four measurements in the controlled variables. The optimal CV's using single measurements and measurement combinations of three and four measurements are presented in Table 7.1. The maximum loss in hours is included in the rightmost

column.

Table 7.1: Optimal Controlled Variables

Description	CV's (CV ₁ on top, CV ₂ on bottom)	Max. loss
4 measurements	$0.70 R + 0.52 T + 0.50 W - 0.01 N$ $-0.19 R + 0.76 T - 0.36 W + 0.50 N$	2.02
3 measurements	$0.83 R + 0.56 T - 0.05 N$ $-0.51 R + 0.64 T + 0.58 N$	3.15
Single measurements	W P	6.24
Constant Inputs	W N	11.44

For single measurement controlled variables, the results show that it is optimal to control the topdrive power by manipulating the drill string rotational speed, and keep the weight on bit (WOB) constant. Combining several measurements will give a lower loss, but the loss is small (approximately 1 % of the active drilling time) and the complexity of the control structure will increase.

A constant input policy will only have a loss of approximately 1 % of the active drilling time compared to the optimal single measurement control structure, thus raising the question of whether or not implementing a control structure is worth the added complexity to the drilling system. However, problems with stick-slip phenomenon are prone in drilling systems operating with a constant drill string rotational speed. Several authors have proposed stick-slip prevention techniques involving a varying rotational drill string speed. Therefore, it is likely that a control structure a varying drill string RPM will be optimal.

7.1.2 Pressure Control & Automation

A feedback control structure involving PI controllers was designed for controlling the bottom hole pressure, using the back pressure pump and the choke valve opening as manipulated inputs. The time spent performing pipe connections and drilling trips is an important factor in the optimization of the drilling process. It is important that these procedures are performed as fast as possible, while keeping the bottom hole pressure within its margins. Procedures that involve room for automation are the ramping down/up of the main mud pump, as well as tripping the drill string in and out of the well. An automatic control system was designed to perform these procedures as fast as possible, while keeping the bottom hole pressure within a pressure window of ± 5 bar. The control structure was able to perform the tasks at speeds that are likely to be close to the physical limitations of the process equipment. Thus, we may conclude that the performance is satisfactory.

An alternative solution of implementing a model predictive controller was discussed. The MPC will perform as a supervisory controller in a hierarchical structure. An MPC will give superior results compared to a stand-alone regulatory control structure, but requires an increased modeling effort and is more error prone.

7.2 Further work

The drilling process involves many challenges and complications that make it difficult to assess the process completely and take everything into account. The thesis work has been carried out without any prior experience with drilling processes, thus consisting of rather simplified models. Further studies of the drilling process and industry experience would undoubtedly result in a more detailed drilling model, improving the accuracy of the results.

It would be interesting to test the model and results of this thesis in real-life drilling operations. A brute-force analysis should be performed, implementing control of the self-optimizing controlled variables determined in this thesis. The results would show whether or not the theoretical results hold for a real-life drilling scenario. Similarly, the real-life performance of the suggested feedback pressure control structure should be tested.

The results will also show whether the simple steady-state model is adequate in describing the drilling process. In case improvements are required, the results may give insight to which areas of the model are weaker, and which are stronger.

Bibliography

- [1] World Energy Outlook. International Energy Agency, 2009.
- [2] Øyvind N. Starnes. Adaptive observer for bottomhole pressure during drilling. M. Sc. thesis, NTNU, Department of Engineering Cybernetics, 2007.
- [3] Mark S. Gockenbach. Lecture: Introduction to sequential quadratic programming. Michigan Technological University, <http://www.math.mtu.edu/~msgocken/ma5630spring2003/lectures/sqp1/sqp1.pdf>.
- [4] Moritz Kuhn. The Karush-Kuhn-Tucker Theorem. CDSEM Uni Mannheim, 2006.
- [5] Sigurd Skogestad and Ian Postlethwaite. *Multivariable Feedback Control: Analysis and Design*. John Wiley & Sons, Ltd, second edition, 2005.
- [6] Sigurd Skogestad. Control structure design for complete chemical plants. *Computers and Chemical Engineering*, 28:219–234, 2004.
- [7] Sigurd Skogestad. Plantwide control: the search for the self-optimizing control structure. *Journal of Process Control*, 10:487–507, 2000.
- [8] Vidar Alstad, Sigurd Skogestad, and Eduardo S. Hori. Optimal measurement combinations as controlled variables. *Journal of Process Control*, 19:138–148, 2009.
- [9] Ivar J. Halvorsen, Sigurd Skogestad, John C. Morud, and Vidar Alstad. Optimal Selection of Controlled Variables. *Industrial Engineering Chemistry Research*, 42(14):3273–3284, 2003.
- [10] Vidar Alstad and Sigurd Skogestad. Null Space Method for Selecting Optimal Measurement Combinations as Controlled Variables. *Industrial Engineering Chemistry Research*, 46:846–853, 2007.
- [11] Ramprasad Yelchuru, Sigurd Skogestad, and Henrik Manum. MIQP formulation for Controlled Variable Selection in Self Optimizing Control. Submitted to DYCOPS 2010 Symposium, 2010.
- [12] A. T. Bourgoyne and F. S. Young. A multiple regression approach to optimal drilling and abnormal pressure detection. *Society of Petroleum Engineers (SPE) Journal*, pages 371–384, Aug. 1974.
- [13] A.T. Bourgoyne, M.E. Chenevert, K.K. Millheim, and F.S. Young. *Applied Drilling Engineering*. Society of Petroleum Engineering (SPE), 1986.
- [14] P. L. Moore. *Drilling Practices Manual*. Petroleum Publishing Company, Tulsa, OK, U.S.A., 1974.

- [15] S. F. Chien. Annular Velocity for Rotary Drilling Operations. In *Proceedings of SPE Fifth Conference on Drilling and Rock Mechanics, Jan. 5-6, 1971*, pages 5–16. Society of Petroleum Engineers (SPE), Austin, TX, U.S.A., 1971.
- [16] MATLAB R2009a Documentation. The MathWorks, Inc., 2009.
- [17] D. E. Seborg, T. F. Edgar, and D. A. Mellichamp. *Process Dynamics and Control*. John Wiley & Sons, Ltd, second edition, 2004.
- [18] Ronald L. Reed. A Monte Carlo Approach to Optimal Drilling. *Society of Petroleum Engineers (SPE) Journal*, 12(5):423–438, 1972.
- [19] E. M. Galle and H. B. Woods. Best Constant Weight and Rotary Speed for Rotary Rock Bits. *Drilling and Production Practice*, pages 48–73, 1963.
- [20] John-Morten Godhavn. Control requirements for high-end automatic MPD operations. SPE/IADC Drilling Conference and Exhibition, 17-17 March 2009, Amsterdam, The Netherlands, 2009.
- [21] Tuna Eren and M. Evren Ozbayoglu. Real Time Optimization of Drilling Parameters During Drilling Operations. SPE Oil and Gas India Conference and Exhibition, 20-22 January 2010, Mumbai, India, 2010.
- [22] Eva María Navarro-López and Rodolfo Suárez. Practical approach to modelling and controlling stick-slip oscillations in oilwell drillstrings. In *Proceedings of the 2004 IEEE International Conference on Control Applications, 2-4 September*. Institute of Electrical and Electronics Engineers (IEEE), Taipei, Taiwan, 2004.
- [23] Ahmet S. Yigit and Andreas P. Christoforou. Stick-Slip and Bit-Bounce Interaction in Oil-Well Drillstrings. *Journal of Energy Resources Technology*, 128:268–274, December 2006.
- [24] F. Abdulgalil and H. Siguerdidjane. Nonlinear Friction Compensation Design for Suppressing Stick Slip Oscillations in Oil Well Drillstrings. In *Proceedings of DYCOPS 7, 5-7 July, 2004*. International Federation of Automatic Control (IFAC), Cambridge, MA, U.S.A., 2004.
- [25] R. W. Tucker and C. Wang. On the Effective Control of Torsional Vibrations in Drilling Systems. *Journal of Sound and Vibration*, 244(1):101–122, 1999.
- [26] G. W. Halsey, A. Kyllingstad, and A. Kylling. Torque Feedback Used to Cure Slip-Stick Motion. In *Proceedings of the 63rd SPE Annual Technical Conference and Exhibition, 2-5 October, 1988*. Society of Petroleum Engineers (SPE), Houston, TX, U.S.A., 1988.
- [27] Kazem Javanmardi and D. T. Gaspard. Application of Soft-Torque Rotary Table in Mobile Bay. SPE/IADC Drilling Conference, 18-21 February, New Orleans, LA, U.S.A., 1992.
- [28] R. I. Leine. Literature Survey on Torsional Drillstring Vibrations. Internal Report - Division of Computational and Experimental Mechanics, Department of Mechanical Engineering, Eindhoven University of Technology, Eindhoven, The Netherlands, 1997.
- [29] Glenn-Ole Kaasa. A Simple Dynamic Model of Drilling for Control. Technical Report, Statoil Research Centre, Porsgrunn, Norway, 2007.
- [30] G. Nygaard, M. Nikolaou, E. H. Vefring, H. Siahaan, and Ø . Breyholtz. Control Hierarchy for Automated Co-ordinated Control of Drilling Equipment. Report - International Research Institute of Stavanger (IRIS), 2010.

- [31] Øyvind Nistad Stamnes, Jing Zhou, Glenn-Ole Kaasa, and Ole Morten Aamo. Adaptive observer design for the bottomhole pressure of a managed pressure drilling system. In *Proceedings of 47th IEEE Conference on Decision and Control, 9-11 December*, pages 2961–2966. Institute of Electrical and Electronics Engineers (IEEE), Cancun, Mexico, 2008.
- [32] B. Wayne Bequette. *Process Control: Modeling, Design and Simulation*. Prentice Hall, 2003.
- [33] Øyvind Breyholtz, Gerhard Nygaard, Hardy Siahaan, and Michael Nikolaou. Managed Pressure Drilling: A Multi-Level Control Approach. SPE Intelligent Energy Conference and Exhibition, 23-25 March 2010, Utrecht, The Netherlands, 2010.

Appendix A

Nomenclature

Table A.1: Nomenclature

Symbol	Description	Unit
β	Bulk modulus	<i>bar</i>
μ	Viscosity	<i>Pa·s</i>
ρ_f	Effective mud density	<i>kg/m³</i>
ρ / ρ_m	Mud density	<i>kg/m³</i>
ρ_s	Formation density	<i>kg/m³</i>
θ_1	Annulus friction parameter	<i>kg/m⁴ s</i>
θ_2	Drill string friction parameter	<i>kg/m⁷</i>
A_a	Cross-sectional area of annulus	<i>m²</i>
D	Well depth	<i>m</i>
d_b	Drill bit diameter	<i>m</i>
d_H	Hydraulic diameter	<i>m</i>
d_i	Drill string inner diameter	<i>m</i>
d_p	Drilled particle diameter	<i>m</i>
d_s	Drill string outer diameter	<i>m</i>
F_{bo}	Buoyant force	<i>N</i>
F_c	Cutting force	<i>N</i>
F_g	Gravitational force	<i>N</i>
F_j	Hydraulic jet impact force	<i>N</i>
f	Friction factor	-
g	Acceleration due to Earth gravity	<i>m/s²</i>
$J(u, d)$	Objective function value	<i>hours</i>
K	Bit life-time constant	<i>hours</i>
K_c	Valve flow constant	<i>m²</i>
k_c^0	Specific cutting force constant	<i>N/ton m²</i>
k_c	Specific cutting force	<i>N/m²</i>
M	Mass coefficient	<i>10⁵ kg/m⁴</i>
N_{Re}	Reynolds number	-
N	Drill string rotational speed	<i>min⁻¹</i>
P	Power	<i>kW</i>
p_{bh}	Bottom hole pressure	<i>bar</i>

Continued on next page

Table A.1 – continued from previous page

Symbol	Description	Unit
p_c	Choke pressure	<i>bar</i>
p_f	Formation pressure	<i>bar</i>
q_{bit}	Mud flow rate at drill bit	<i>liter/s</i>
q_{in}	Main mud pump flow rate	<i>liter/s</i>
q_s	Feed of cuttings	m^3/s
R	Rate of penetration	<i>m/hr</i>
R_0	Drillability constant	<i>m/hr</i>
T	Torque	<i>kN/m</i>
t_c	Total connection time	<i>hours</i>
t_c^0	Single connection time	<i>hours</i>
t_d	Drilling time	<i>hours</i>
t_d^0	Drill bit life-time	<i>hours</i>
t_t	Total trip time	<i>hours</i>
t_t^0	Single trip time	<i>hours</i>
v_{sl}	Particle slip velocity	<i>m/s</i>
v_a	Annulus velocity	<i>m/s</i>
V_a	Annulus volume	m^3
V_d	Internal volume of drill string	m^3
V_s	Volume of drilled particle	m^3
v_T	Transport velocity	<i>m/s</i>
W	Weight on bit	<i>tons</i>
x_c	Fraction of cuttings in mud	%
z_c	Choke valve opening	%

Appendix B

Miscellaneous Calculation Matrices

The gain matrix, sensitivity matrix and various other matrices used in the calculations are presented below.

$$\nabla^2 J(u) = J_{uu} = \begin{bmatrix} 1.88160.1159 \\ 0.11590.0222 \end{bmatrix}$$

$$G = \begin{bmatrix} 0.5046 & 0.1056 \\ 0.9975 & 0 \\ 10.4167 & 3.4536 \\ 0.0331 & 0.0069 \\ 1.0000 & 0 \\ 0 & 1.0000 \end{bmatrix}$$

$$S_1 = \begin{bmatrix} 0.1005 & 0 & 0 & 0 & 0 & 0 \\ 0 & 0.0505 & 0 & 0 & 0 & 0 \\ 0 & 0 & 0.0102 & 0 & 0 & 0 \\ 0 & 0 & 0 & 0.8727 & 0 & 0 \\ 0 & 0 & 0 & 0 & 0.2888 & 0 \\ 0 & 0 & 0 & 0 & 0 & 0.0241 \end{bmatrix}$$

$$G' = S_1 G = \begin{bmatrix} 0.05 & 0.01 \\ 0.05 & 0 \\ 0.11 & 0.04 \\ 0.03 & 0.01 \\ 0.29 & 0 \\ 0 & 0.02 \end{bmatrix}$$

$$F = \begin{bmatrix} 3.94 & 0.00 & -0.15 \\ -6.71 & -0.00 & -0.00 \\ -27.05 & 0.00 & 0.00 \\ 0.26 & 0.00 & -0.01 \\ -0.18 & -0.00 & -0.00 \\ 12.60 & 0.00 & 0.00 \end{bmatrix}$$

$$W_d = \begin{bmatrix} -2.5 & 0 & 0 \\ 0 & 500 & 0 \\ 0 & 0 & 10 \end{bmatrix}$$

$$W_n = \begin{bmatrix} 0.1 & 0 & 0 & 0 & 0 & 0 \\ 0 & 3 & 0 & 0 & 0 & 0 \\ 0 & 0 & 30 & 0 & 0 & 0 \\ 0 & 0 & 0 & 0.5 & 0 & 0 \\ 0 & 0 & 0 & 0 & 3 & 0 \\ 0 & 0 & 0 & 0 & 0 & 10 \end{bmatrix}$$

$$\tilde{F} = [F W_d \ W_n] = \begin{bmatrix} -9.85 & 0.00 & -1.47 & 0.1 & 0 & 0 & 0 & 0 & 0 \\ 16.78 & -0.00 & -0.00 & 0 & 3 & 0 & 0 & 0 & 0 \\ 67.63 & 0.00 & 0.00 & 0 & 0 & 30 & 0 & 0 & 0 \\ -0.65 & 0.08 & -0.10 & 0 & 0 & 0 & 0.5 & 0 & 0 \\ 0.46 & -0.00 & -0.00 & 0 & 0 & 0 & 0 & 3 & 0 \\ -31.49 & 0.00 & 0.00 & 0 & 0 & 0 & 0 & 0 & 10 \end{bmatrix}$$

Appendix C

Solving the Exact Local Method for a Multivariable Case

The following method was used to solve the exact local method in Chapter 5. The material was originally produced by Alstad et. al. [8]. The presented material considers a system with two controlled variables (and manipulated variables), but could just as well be extended to any dimension.

The minimization problem encountered in solving the exact local method is presented in Equation C.1.

$$\min_H \|H\tilde{F}\|_2^2 \quad (\text{C.1})$$

$$\text{subject to: } HG = J_{uu}^{1/2}$$

In order to solve the exact local method, we transform the multivariable case into a scalar problem. We introduce the matrix $X = H^T$, and further split the matrices X and $J_{uu}^{1/2}$ into the vectors as shown in Equation C.2.

$$X = [x_1 \quad x_2] \quad J_{uu}^{1/2} = [J_1 \quad J_2] \quad (\text{C.2})$$

The long vectors x_n and J_n , and the large matrices G_n^T and \tilde{F}_n are introduced as presented in Equations C.3 and C.4.

$$x_n = \begin{bmatrix} x_1 \\ x_2 \end{bmatrix}, \quad J_n = \begin{bmatrix} J_1 \\ J_2 \end{bmatrix} \quad (\text{C.3})$$

$$G_n^T = \begin{bmatrix} G^T & 0 \\ 0 & G^T \end{bmatrix} \quad \tilde{F}_n = \begin{bmatrix} \tilde{F} & 0 \\ 0 & \tilde{F} \end{bmatrix} \quad (\text{C.4})$$

Applying the equations above to $\|H\tilde{F}\|_2$, we can write Equation C.5 for the objective function

of the minimization problem.

$$\|H\tilde{F}\|_2^2 = \left\| \begin{bmatrix} x_1^T \tilde{F} \\ x_2^T \tilde{F} \end{bmatrix} \right\|_2^2 = \| [x_1^T \tilde{F} \quad x_2^T \tilde{F}] \|_2^2 \quad (\text{C.5})$$

$$= \|x_n^T \tilde{F}_n\|_2^2 = \|\tilde{F}_n^T x_n\|_2^2 = x_n^T \tilde{F}_n \tilde{F}_n^T x_n \quad (\text{C.6})$$

Since J_{uu} is a symmetric positive definite matrix at an unconstrained optimum, $J_{uu}^{1/2}$ is also a symmetric positive definite matrix. Thus, we can write $HG = G^T H^T = G^T X = J_{uu}^{1/2}$.

Further:

$$G^T X = [G^T x_1 \quad G^T x_2] = [J_1 \quad J_2]$$

Thus, the constraints may be written as shown in Equation C.7.

$$\begin{bmatrix} G^T x_1 \\ G^T x_2 \end{bmatrix} = [J_1 J_2] \Rightarrow G_n x_n = J_n \quad (\text{C.7})$$

The result is that the optimization problem in Equation C.1 may be re-written as Equation C.8 and the quadratic program can easily be solved, e.g. using the MATLAB[®] function *quadprog*.

$$\min_{x_n} x_n^T \tilde{F}_n \tilde{F}_n^T x_n \quad (\text{C.8})$$

subject to: $G_n x_n = J_n$

The x_n matrix is finally reshaped back to form the optimal measurement combination matrix H , where the first row of H is found as the top half of the column vector x_n while the second row of H is the bottom part.

$$H = \begin{bmatrix} x_1^T \\ x_2^T \end{bmatrix}$$

Appendix D

Results of the Exact Local Method

The results of the exact local method for 2-6 measurement combinations are presented in Tables D.1 through D.5.

Table D.1: Optimal Combinations of 6 Measurements

H matrix						Max. loss
0.75	0.40	0.02	0.00	0.53	-0.07	1.87
-0.39	-0.11	0.16	-0.00	-0.77	0.46	

Table D.2: Optimal Combinations of 5 Measurements

H matrix						Max. loss
0.00	0.02	0.01	0.83	0.55	0.01	4.83
0.00	0.04	0.10	-0.64	-0.72	0.24	
0.58	0.00	0.04	0.00	0.80	-0.14	2.71
-0.32	0.00	0.15	-0.00	-0.81	0.46	
0.70	0.52	0.00	0.00	0.50	-0.01	2.02
-0.19	0.76	0.00	-0.00	-0.36	0.50	
0.75	0.40	0.02	0.00	0.53	-0.07	1.87
-0.39	-0.11	0.16	0.00	-0.77	0.46	
0.88	0.47	0.01	0.00	0.00	-0.10	3.04
-0.81	-0.37	0.13	-0.00	0.00	0.44	
0.62	0.49	-0.00	0.00	0.61	0.00	2.27
0.12	-0.49	0.15	0.00	-0.85	0.00	

Table D.3: Optimal Combinations of 4 Measurements

H matrix						Max. loss
0.00	0.00	0.01	0.82	0.57	0.01	4.85
0.00	0.00	0.10	-0.68	-0.69	0.23	
0.00	0.09	0.00	0.83	0.55	0.03	4.97
0.00	0.69	0.00	-0.41	-0.46	0.39	
0.00	0.01	0.01	0.00	1.00	0.03	5.13
0.00	0.06	0.12	0.00	-0.94	0.30	
0.00	0.03	0.00	1.00	0.00	-0.00	56.28
0.00	-0.03	0.01	-1.00	0.00	0.03	
0.00	-0.01	0.01	0.85	0.53	0.00	4.86
0.00	-0.58	0.15	0.39	-0.70	0.00	
-0.06	0.00	0.00	-0.00	1.00	0.06	8.50
-0.70	0.00	0.00	-0.00	0.62	0.35	
0.58	0.00	0.04	0.00	0.80	-0.14	2.71
-0.32	0.00	0.15	0.00	-0.81	0.46	
0.96	0.00	0.06	0.00	0.00	-0.27	6.04
-0.82	0.00	0.10	-0.00	0.00	0.56	
0.12	0.00	0.02	0.00	0.99	0.00	4.41
0.38	0.00	0.08	0.00	-0.92	0.00	
0.70	0.52	0.00	0.00	0.50	-0.01	2.02
-0.19	0.76	0.00	0.00	-0.36	0.50	
0.83	0.56	0.00	0.00	0.00	-0.05	3.15
-0.51	0.64	0.00	-0.00	0.00	0.58	
0.62	0.48	0.00	0.00	0.62	0.00	9.66
0.54	0.41	0.00	0.00	-0.74	0.00	
0.88	0.47	0.01	0.00	0.00	-0.10	3.04
-0.81	-0.37	0.13	0.00	0.00	0.44	
0.62	0.49	-0.00	0.00	0.61	0.00	2.27
0.12	-0.49	0.15	0.00	-0.85	0.00	
0.75	0.66	-0.01	0.00	0.00	0.00	4.61
-0.42	-0.90	0.14	-0.00	0.00	0.00	

Table D.4: Optimal Combinations of 3 Measurements

H matrix						Max. loss
0.00	0.00	0.00	-0.46	0.89	0.05	10.31
0.00	0.00	0.00	-1.00	0.05	0.04	
0.00	0.00	0.01	0.00	1.00	0.02	5.13
0.00	0.00	0.13	0.00	-0.95	0.29	
0.00	0.00	0.00	1.00	0.00	-0.02	60.89
0.00	0.00	0.00	-1.00	0.00	0.04	
0.00	0.00	0.01	0.90	0.44	0.00	4.87
0.00	0.00	0.01	0.99	-0.14	0.00	
0.00	0.12	0.00	0.00	0.99	0.06	5.27
0.00	0.75	0.00	0.00	-0.51	0.41	
0.00	0.05	0.00	1.00	0.00	-0.00	56.74
0.00	0.05	0.00	-1.00	0.00	0.06	
0.00	0.03	0.00	1.00	0.03	0.00	107.64
0.00	0.03	0.00	1.00	-0.05	0.00	
0.00	1.00	0.05	0.00	0.00	-0.08	160.09
0.00	-0.85	0.13	0.00	0.00	0.51	
0.00	-0.07	0.02	0.00	1.00	0.00	5.20
0.00	-0.64	0.16	0.00	-0.75	0.00	
0.00	0.05	-0.00	1.00	0.00	0.00	57.37
0.00	-0.11	0.02	-0.99	0.00	0.00	
-0.06	0.00	0.00	0.00	1.00	0.06	8.50
-0.70	0.00	0.00	0.00	0.62	0.35	
0.99	0.00	0.00	0.00	0.00	-0.10	165.27
0.68	0.00	0.00	0.00	0.00	0.73	
0.49	0.00	0.00	0.00	0.87	0.00	84.74
0.86	0.00	0.00	0.00	-0.52	0.00	
0.96	0.00	0.06	0.00	0.00	-0.27	6.04
-0.82	0.00	0.10	0.00	0.00	0.56	
0.12	0.00	0.02	0.00	0.99	0.00	4.41
0.38	0.00	0.08	0.00	-0.92	0.00	
1.00	0.00	-0.04	0.00	0.00	0.00	2077.66
-1.00	0.00	0.07	-0.00	0.00	0.00	
0.83	0.56	0.00	0.00	0.00	-0.05	3.15
-0.51	0.64	0.00	0.00	0.00	0.58	
0.62	0.48	0.00	0.00	0.62	0.00	9.66
0.54	0.41	0.00	0.00	-0.74	0.00	
0.49	0.87	0.00	0.00	0.00	0.00	227.97
0.86	-0.52	0.00	0.00	0.00	0.00	
0.75	0.66	-0.01	0.00	0.00	0.00	4.61
-0.42	-0.90	0.14	0.00	0.00	0.00	

Table D.5: Optimal Combinations of 2 Measurements

H matrix						Max. loss
0.00	0.00	0.00	0.00	1.00	0.06	11.44
0.00	0.00	0.00	0.00	0.49	0.87	
0.00	0.00	0.00	1.00	0.00	-0.00	475.95
0.00	0.00	0.00	1.00	0.00	0.04	
0.00	0.00	0.00	1.00	0.06	0.00	184.94
0.00	0.00	0.00	1.00	-0.02	0.00	
0.00	0.00	0.33	0.00	0.00	-0.94	168.84
0.00	0.00	0.07	0.00	0.00	1.00	
0.00	0.00	0.02	0.00	1.00	0.00	6.24
0.00	0.00	0.12	0.00	-0.99	0.00	
0.00	0.00	-0.00	1.00	0.00	0.00	3790.86
0.00	0.00	0.00	-1.00	0.00	0.00	
0.00	1.00	0.00	0.00	0.00	0.06	161.90
0.00	0.49	0.00	0.00	0.00	0.87	
NaN	NaN	NaN	NaN	NaN	NaN	NaN
NaN	NaN	NaN	NaN	NaN	NaN	
0.00	0.06	0.00	1.00	0.00	0.00	278.10
0.00	-0.02	0.00	1.00	0.00	0.00	
0.00	1.00	0.02	0.00	0.00	0.00	160.70
0.00	-0.99	0.12	0.00	0.00	0.00	
0.99	0.00	0.00	0.00	0.00	-0.10	165.27
0.68	0.00	0.00	0.00	0.00	0.73	
0.49	0.00	0.00	0.00	0.87	0.00	84.74
0.86	0.00	0.00	0.00	-0.52	0.00	
0.03	0.00	0.00	-1.00	0.00	0.00	NaN
-0.03	0.00	0.00	1.00	0.00	0.00	
1.00	0.00	-0.04	0.00	0.00	0.00	2077.66
-1.00	0.00	0.07	0.00	0.00	0.00	
0.49	0.87	0.00	0.00	0.00	0.00	227.97
0.86	-0.52	0.00	0.00	0.00	0.00	

Appendix E

MATLAB files

The MATLAB scripts and functions that were used in order to produce the results of this thesis work are attached on the CD-ROM marked *Appendix E*. A list of the file names and descriptions are presented in Table E.1.

Table E.1: List of MATLAB Files

File name	Description
main4u.m	Main script for optimizing the drilling process with 4 inputs
drilling4u.m	Steady-state drilling model accepting 4 inputs
drillsolve4u.m	Function used to solve equation system in drilling4u.m
objfun4u.m	Objective function accepting 4 inputs
constraints.m	Drilling model constraints
main.m	Main script for optimizing the unconstrained drilling process with 2 inputs
drilling.m	Steady-state drilling model accepting 2 inputs
drillsolve.m	Function used to solve equation system in drilling.m
objfun.m	Objective function accepting 2 inputs
msv.m	Function used to solve the method of maximizing the minimum singular value
exactlocal.m	Function used to solve the exact local method
runSim.m	Main script for running control simulations on dynamic pressure model
calcf.m	Function used to calculate the dynamics of the pressure model

main4u.m:

```

1  %Script for optimizing the drilling process with 4 inputs
2  %Needs external functions drilling4u.m, drillsolve4u.m
3  %objfun4u.m and constraints.m.
4  %DEH - 2010
5
6  clear all
7  close all
8  clc
9
10 global db Wdbmax tt0 dstring Wdbt R0 K kc D dp Aa g rho rhos thetal
11
12 %Parameters:
13 db = 0.254; %Bit diameter, m
14 Wdbmax = 178.583; %Maximum WOB per m diameter, tons/m
15 tt0 = 10; %Trip time, hours
16 dstring = 0.1; %Diameter of drill string, m
17 D = 3000; %Depth, m
18 Aa = (db^2-dstring^2)*pi/4; %Cross-sectional area of annulus, m2
19 g = 9.81; %Gravity
20 R0 = 5; %Formation drillability, m/hr
21 tempR0 = R0;
22 K = 15*R0; %Formation abrasiveness constant, hours
23 kc = 5e5/R0; %Specific cutting force, N/m2-ton
24 Wdbt = 63/R0; %Threshold WOB per m diameter, tons/m
25 thetal = 900; %Friction parameter
26 rhos = 2700; %Formation density, kg/m3
27 rho = 1400; %Mud density, kg/m3
28 dp = 0.005; %Particle diameter, m
29
30 %Optimization:
31 u0 = [30; %WOB, tons
32       100; %RPM
33       40; %qmud, l/s
34       10]; %pc, bar
35
36 lb = [0; 0; 0; 0];
37 ub = [Wdbmax*db; 200; 50; 100];
38 options = optimset('Display','iter','TolFun',1e-12,'MaxFunEvals',300);
39 [u,fval,exitflag,output,lambda,grad,hessian] = fmincon(@objfun4u, u0,...
40     [],[],[],[],lb,ub,@constraints,options)
41 Juu = hessian;
42
43 %Nominal optimum u and y:
44 y0 = drilling4u(u)

```

drilling4u.m:

```

1 function y = drilling4u(u)
2 %Function that calculates drilling model equations.
3 %Run main4u.m
4 %DEH - 2010
5
6 global db dstring kc WOB RPM qmud pc
7
8 y = zeros(9,1);
9
10 WOB = u(1);
11 RPM = u(2);
12 qmud = u(3);
13 pc = u(4);
14
15 x0 = [15;1;460];
16 res = fsolve(@drillsolve4u,x0);
17 y(1) = res(1); %ROP
18 y(4) = res(2); %Cuttings fraction
19 y(5) = res(3); %Mud flow
20 F = u(1)/db*kc*db^2*pi/4; %Force, N, function of WOB and formation strength
21 y(2) = F*dstring/2000; %Torque, kNm.
22 y(3) = y(2)*2*pi*u(2)/60; %Power, kW
23 y(6) = u(1);
24 y(7) = u(2);
25 y(8) = u(3);
26 y(9) = u(4);

```

drillsolve4u.m:

```

1 function f = drillsolve4u(y)
2 %Function that solves system of drilling equations.
3 %Run main4u.m
4 %DEH - 2010
5
6 global db Aa dp g Wdbt R0 rho rhos thetal D WOB RPM qmud pc
7
8 f = zeros(3,1);
9
10 newrho = rho*(1-y(2)/100) + rhos*y(2)/100; %rhof, kg/m3
11 bhp = pc + thetal*qmud/1000 + newrho*g*D/1e5; %BHP, bar
12
13 An = 3*pi*0.01^2/4; %nozzle x-sec area, m2
14 Fj = qmud^2*rho/An/1e6; %hydraulic jet impact force, N
15 ROP = R0*(WOB/db-Wdbt)/(71.433-Wdbt)*(RPM/60)^0.7*exp(0.01*...
16     (470-bhp))*(Fj/4448.22)^.3;
17
18 va = qmud/1000/Aa; %annulus velocity, m/s
19 vslip = sqrt(8/9*g*dp*(rhos-newrho)/rho); %slip velocity, m/s
20 vT = va - vslip; %transport velocity, m/s
21 qs = ROP*pi/4*db^2*1000/3600; %cuttings feed rate, l/s
22 xc = qs/1000/Aa/vT*100; %cuttings fraction
23
24 f(1) = ROP - y(1);
25 f(2) = xc - y(2);
26 f(3) = bhp - y(3);

```

objfun4u.m:

```

1 function f = objfun4u(u)
2 %Objective function for optimization of the drilling process.
3 %Run main4u.m
4 %DEH
5
6 global db Wdbmax tt0 K D
7
8 y = drilling4u(u);
9 R = y(1);
10
11 td0 = K*(60/u(2))^1.7*(Wdbmax-u(1)/db)/(Wdbmax-71.433); %bit life-time
12 f = D*(1/R + tt0/(R*td0)); %J, objective function

```

constraints.m:

```

1 function [C Ceq] = constraints(x)
2 %Function containing the drilling process constraints.
3 %Run main4u.m
4 %DEH - 2010
5
6 y = drilling4u(x);
7
8 Ceq = []; %no equality constraints
9 C = zeros(2,1);
10
11 C(1) = 470 - y(5);
12 C(2) = y(5) - 480;

```

main.m:

```

1 %Script for optimizing drilling process with 2 inputs
2 %Needs external functions drilling.m, drillsolve.m, objfun.m
3 %msv.m and exactlocal.m.
4 %DEH - 2010
5
6 clear all
7 close all
8 clc
9
10 global db Wdbmax tt0 dstring Wdbt R0 K kc D bhp qmud dp Aa g rho rhos
11
12 %Parameters:
13 db = 0.254; %Bit diameter, m
14 Wdbmax = 178.583; %Maximum WOB per m diameter, tons/m
15 tt0 = 10; %Trip time, hours
16 dstring = 0.1; %Diameter of drill string, m
17 D = 3000; %Depth
18 Aa = (db^2-dstring^2)*pi/4; %Cross-sectional area of annulus, m2
19 g = 9.81; %Gravity
20 R0 = 5; %Formation drillability, m/hr
21 tempR0 = R0;
22 K = 15*R0; %Formation abrasiveness constant, hours
23 kc = 5e5/R0; %Specific cutting force, N/m2-ton
24 Wdbt = 63/R0; %Threshold WOB per m diameter, tons/m

```

```

25 bhp = 470; %BHP, bar
26 bhpsave = bhp;
27 qmud = 50; %Mud flow rate, l/s
28 rhos = 2700; %Formation density, kg/m3
29 rho = 1400; %Mud density, kg/m3
30 dp = 0.005; %Diameter of drilled particle, m
31
32 %Optimization:
33 u0 = [30; %WOB, tons
34       100]; %RPM
35 lb = [0; 0];
36 ub = [Wdbmax*db; 300];
37 options = optimset('Display','iter','TolFun',1e-12,'MaxFunEvals',300);
38 [u,fval,exitflag,output,lambda,grad,hessian] = fmincon(@objfun, u0,[],...
39             [],[],[],lb,ub,[],options);
40 Juu = hessian;
41
42 %Nominal optimum u and y:
43 y0 = drilling(u);
44
45 %Gains:
46 G = zeros(length(y0),length(u));
47 Δu = 0.01*u;
48 for i = 1:length(u)
49     udev = u+Δu.*[zeros(i-1,1); ones(1,1); zeros(length(u)-i,1)];
50     G(:,i) = (drilling(udev) - y0)./(Δu(i));
51 end
52 [ny,nu] = size(G);
53
54 %Implementation errors:
55 eimp = [0.1; 3; 30; 0.5; 3; 10];
56
57 %Disturbances:
58 d = [R0;rhos;bhp];
59 nd = length(d);
60 Δyopt = zeros(length(y0),nd);
61 Gd = zeros(length(y0),nd);
62 F = zeros(length(y0),nd);
63 Δd = 0.01*d;
64 for i = 1:nd
65     ddev = d+Δd.*[zeros(i-1,1);ones(1,1);zeros(nd-i,1)];
66     R0 = ddev(1);
67     K = 15*R0;
68     kc = 5e5/R0;
69     Wdbt = 63/R0;
70     rhos = ddev(2);
71     bhp = ddev(3);
72     Gd(:,i) = (drilling(u)-y0)/Δd(i);
73
74     %Re-optimization
75     options = optimset('TolFun',1e-12,'MaxFunEvals',300);
76     [uopt,fvalopt,exitflag,output] = fmincon(@objfun, u0,[],[],[],[],...
77         lb,ub,[],options);
78     Δyopt(:,i) = drilling(uopt)-y0;
79     F(:,i) = Δyopt(:,i)/Δd(i);
80 end
81 bhp = bhpsave;
82
83 stepsize = 0.1;
84 lossplot = zeros(1+ny+nchoosek(ny,nu)+nchoosek(ny,nu+1)+...
85               nchoosek(ny,nu+2),1/stepsize+1);

```

```

86
87 for a = -1:stepsize:1
88     c = (1+stepsize+a)/stepsize;
89     ddash = a*ones(nd);
90     ndash = a*ones(ny);
91     Wd = diag([-2.5; 500; 10]).*ddash;
92     Wn = diag(eimp).*ndash;
93     Ftilde = [F*Wd Wn];
94
95     %Exact Local Method:
96     tempG = G;
97     tempGd = Gd;
98     tempFtilde = Ftilde;
99     H1 = zeros(size(lossplot,1),ny);
100    H2 = zeros(size(lossplot,1),ny);
101    lossvector = zeros(size(lossplot,1),2);
102    [H maxloss] = exactlocal(Ftilde,Juu,G,Gd);
103    H1(1,:) = H(1,:);
104    H2(1,:) = H(2,:);
105    lossvector(1,:) = maxloss;
106
107    for i=1:ny
108        G(i,:) = 0;
109        Gd(i,:) = 0;
110        Ftilde(i,:) = 0;
111        [H maxloss] = exactlocal(Ftilde,Juu,G,Gd);
112        H1(i+1,:) = H(1,:);
113        H2(i+1,:) = H(2,:);
114        lossvector(i+1,:) = maxloss;
115        G = tempG;
116        Gd = tempGd;
117        Ftilde = tempFtilde;
118    end
119    n = ny+2;
120    for j = nchoosek(1:ny,nu)'
121        G(j,:) = 0;
122        Gd(j,:) = 0;
123        Ftilde(j,:) = 0;
124        [H maxloss] = exactlocal(Ftilde,Juu,G,Gd);
125        H1(n,:) = H(1,:);
126        H2(n,:) = H(2,:);
127        lossvector(n,:) = maxloss;
128        n = n+1;
129        G = tempG;
130        Gd = tempGd;
131        Ftilde = tempFtilde;
132    end
133    m = n;
134    for j = nchoosek(1:ny,nu+1)'
135        G(j,:) = 0;
136        Gd(j,:) = 0;
137        Ftilde(j,:) = 0;
138        [H maxloss] = exactlocal(Ftilde,Juu,G,Gd);
139        H1(m,:) = H(1,:);
140        H2(m,:) = H(2,:);
141        lossvector(m,:) = maxloss;
142        m = m+1;
143        G = tempG;
144        Gd = tempGd;
145        Ftilde = tempFtilde;
146    end

```

```

147     o = m;
148     for j = nchoosek(1:ny,nu+2) '
149         G(j,:) = 0;
150         Gd(j,:) = 0;
151         Ftilde(j,:) = 0;
152         [H maxloss] = exactlocal(Ftilde,Juu,G,Gd);
153         H1(o,:) = H(1,:);
154         H2(o,:) = H(2,:);
155         lossvector(o,:) = maxloss;
156         o = o+1;
157         G = tempG;
158         Gd = tempGd;
159         Ftilde = tempFtilde;
160     end
161
162     res = [H1 H2 lossvector];
163
164     [C5 I5] = min(res(2:7,13));
165     I5 = I5+1;
166     [C4 I4] = min(res(8:22,13));
167     I4 = I4+7;
168     [C3 I3] = min(res(23:42,13));
169     I3 = I3+22;
170     [C2 I2] = min(res(43:57,13));
171     I2 = I2+42;
172
173     lossplot(:,round(c)) = res(:,13);
174 end
175
176 %Minimum Singular Value method:
177 eopt = max(abs(F*Wd),[],2);
178 span = eopt+eimp;
179 S1 = diag(1./span);
180 SG = S1*G;
181 msvrank = msv(SG,Juu);
182
183 %Nullspace method:
184 nullspaceF = [F(3,1);F(5:6,1)];
185 Hnullspace = null(nullspaceF)';
186
187 lossplot2 = lossplot(:,11:21);
188
189 Hmatrix = zeros(2*size(H1,1),ny);
190 for i = 1:size(H1,1)
191     Hmatrix(2*i-1,:) = H1(i,:);
192     Hmatrix(2*i,:) = H2(i,:);
193 end
194
195 %Results of the exact local method
196 disp(res)
197
198 %Plots
199 x = -1:stepsize:1;
200 x2 = 0:stepsize:1;
201
202 set(0,'defaultaxesfontsize',14);
203 set(0,'defaulttextfontsize',14);
204 set(0,'DefaultLineLineWidth',1.5);
205 set(0,'DefaultFigureColor','none');
206 legFontSize = 14;
207 scrsz = get(0,'ScreenSize');

```

```

208
209 figure('Position',[1 scrsz(4)/2 scrsz(3)/2 scrsz(4)/2])
210 plot(2:6,[lossvector(I2,1),lossvector(I3,1),lossvector(I4,1),...
211     lossvector(I5,1),lossvector(1,1)], 'k')
212 ylabel('Loss = J - Jopt, [hours]')
213 xlabel('No. of measurements')
214 set(gcf, 'PaperPositionMode', 'auto')
215 print -djpeg lossmeas
216
217 figure('Position',[1 scrsz(4)/2 scrsz(3)/2 scrsz(4)/2])
218 plot(x2,lossplot2(1,:), 'k-',x2,lossplot2(I5,:), 'k:',...
219     x2,lossplot2(I4,:), 'k:o',x2,lossplot2(I3,:), 'k-d',...
220     x2,lossplot2(I2,:), 'k-',x2,lossplot2(43,:), 'k-'.')
221 h(1) = legend('R, T, P, x$_c$, W, N', 'R, T, P, W, N', 'R, T, W, N',...
222     'R, T, N', 'P, W', 'W, N (Const. Inputs)', 'Location', 'NorthWest');
223 ylabel('Loss = J - Jopt, [hours]')
224 xlabel('Magnitude of |d| / |n|')
225 set(h, 'Interpreter', 'latex', 'FontSize', legFontSize)
226 set(gcf, 'PaperPositionMode', 'auto')
227 print -djpeg lossbest
228
229 figure('Position',[1 scrsz(4)/2 scrsz(3)/2 scrsz(4)/2])
230 plot(x2,lossplot2(45,:), 'k:*',x2,lossplot2(46,:), 'k-'.',...
231     x2,lossplot2(51,:), 'k-',x2,lossplot2(54,:), 'k:d',...
232     x2,lossplot2(57,:), 'k-')
233 axis([0 1 0 300])
234 h(1) = legend('x$_c$, W', 'P, N', 'T, x$_c$', 'R, W', 'R, T',...
235     'Location', 'NorthWest');
236 ylabel('Loss = J - Jopt, [hours]')
237 xlabel('Magnitude of |d| / |n|')
238 set(h, 'Interpreter', 'latex', 'FontSize', legFontSize)
239 set(gcf, 'PaperPositionMode', 'auto')
240 print -djpeg lossbad

```

drilling.m:

```

1 function y = drilling(u)
2 %Function calculating the drilling equations.
3 %Run script main.m
4 %DEH - 2010
5 global db dstring kc WOB RPM
6
7 y = zeros(6,1);
8
9 WOB = u(1);
10 RPM = u(2);
11
12 x0 = [15; 5];
13 x = fsolve(@drillsolve,x0);
14
15 y(1) = x(1); %ROP, m/hr
16 F = u(1)/db*kc*db^2*pi/4; %Force, N, function of WOB and rock strength
17 y(2) = F*dstring/2000; %Torque, kNm.
18 y(3) = y(2)*2*pi*u(2)/60; %Power, kW
19 y(4) = x(2); %Cuttings percent
20 y(5) = u(1);
21 y(6) = u(2);

```

drillsolve.m:

```

1 function f = drillsolve(y)
2 %Function that solves system of drilling model equations.
3 %Run script main.m.
4 %DEH - 2010
5
6 global db Aa dp g Wdbt R0 rho rhos WOB RPM qmud bhp
7
8 f = zeros(2,1);
9
10 newrho = rho*(1-y(2)/100) + rhos*y(2)/100;
11
12 An = 3*pi*0.01^2/4; %Nozzle x-sec area, m^2
13 Fj = qmud^2*rho/An/1e6; %Hydraulic jet impact force, N
14 ROP = R0*(WOB/db-Wdbt)/(71.433-Wdbt)*(RPM/60)^0.7*exp(0.01*(470-bhp))...
15     *(Fj/4448.22)^.3;
16
17 va = qmud/1000/Aa; %Annulus velocity, m/s
18 vslip = sqrt(8/9*g*dp*(rhos-newrho)/rho); %Slip velocity, m/s
19 vT = va - vslip; %Transport velocity, m/s
20 qs = y(1)*pi/4*db^2*1000/3600; %Cuttings feed rate, l/s
21 xc = qs/1000/Aa/vT*100; %Cuttings percent
22
23 f(1) = ROP - y(1);
24 f(2) = xc - y(2);

```

objfun.m:

```

1 function f = objfun(u)
2 %Objective function for optimization of the drilling process
3 %Run script main.m
4 %DEH - 2010
5
6 global db Wdbmax tt0 K D WOB RPM
7
8 WOB = u(1);
9 RPM = u(2);
10
11 x0 = [15; 5];
12 x = fsolve(@drillsolve,x0);
13
14 R = x(1); %ROP
15 td0 = K*(60/u(2))^1.7*(Wdbmax-u(1)/db)/(Wdbmax-71.433);
16 f = D*(1/R + tt0/(R*td0));

```

msv.m:

```

1 function rank = msv(SG, Juu)
2 %Function that calculates the minimum singular value of combinations
3 %of 2 controlled variables.
4 %Run script main.m
5 %DEH - 2010
6
7 [ny, nu] = size(SG);
8 rank = zeros(nchoosek(ny, nu), nu+1);
9
10 k=1;
11 for a = nchoosek(1:ny, nu) '
12     tempSG = [SG(a(1), :); SG(a(2), :)];
13     minsingval = min(svd(tempSG*inv(sqrtm(Juu))));
14     rank(k, :) = [a(1) a(2) minsingval];
15     k=k+1;
16 end
17
18 rank = sortrows(rank, -3);

```

exactlocal.m:

```

1 function [Hq maxloss] = exactlocal(B, Juu, Gy, Gdy)
2 %Function that solves the exact local method for selection of optimal CV's.
3 %Run script main.m
4 %DEH - 2010
5
6 [ny, nu]= size(Gy);
7 nd = size(Gdy, 2);
8 Juuhalf = sqrtm(Juu);
9 Jn = []; Fn = []; GnyT = [];
10
11 GnyT = zeros(nu*nu, nu*ny);
12 Fn = zeros(nu*ny, nu*(ny+nd));
13 for i = 1:nu
14     GnyT((i-1)*nu+1:i*nu, (i-1)*ny+1:i*ny) = Gy';
15     Jn = [Jn; Juuhalf(i, :)]';
16     Fn((i-1)*ny+1:i*ny, (i-1)*(ny+nd)+1:i*(ny+nd)) = B;
17 end
18
19 if nnz(Gy(:, 1)) == 0 || nnz(Gy(:, 2)) == 0
20     Hq = NaN*ones(nu, ny);
21     maxloss = NaN;
22     avgloss = NaN;
23 else
24     options = optimset('quadprog');
25     options = optimset(options, 'TolPCG', 1e-10, 'TolCon', 1e-10, 'Display', 'iter');
26     xn1 = quadprog(Fn*Fn', zeros(size(Fn*Fn', 1), 1), [], [], GnyT, Jn, [], [], [], options);
27     Hq = reshape(xn1, ny, nu)';
28
29 %normalizing so Euclidean norm of each row = 1
30 Hq = [Hq(1, :)./sqrt(sum(Hq(1, :).^2)); Hq(2, :)./sqrt(sum(Hq(2, :).^2))];
31
32 maxloss = 0.5*norm(sqrtm(Juu)*inv(Hq*Gy)*(Hq*B))^2;
33
34 end

```

runSim.m:

```

1 %Script for simulating performance of an automated pressure control
2 %structure using a simple dynamic pressure model.
3 %Script needs to use external functions calcf.m.
4 %Written by: ?NS 2009
5 %Modified by: DEH 2010
6
7 clear all
8 close all
9 clc
10
11 % set up simulation
12 % stepsize
13 dT = 0.1;
14 % time vector
15 time=0:dT:600;
16
17 % system parameters
18 Va    = 128.45;
19 Vd    = 17.02;
20 VaDot = 0;
21 betaa = 20000;
22 betad = 20000;
23 M     = 8384;
24 rhoa  = 0.0140;
25 rhod  = 0.0140;
26 g     = 9.81;
27 theta1= 900;
28 theta2= 60000;
29 hBit  = 3000;
30 Atot = 0.0485; %Va/hBit + Vd/hBit
31 Apipe = 0.00218; %7" OD 3" ID
32
33 %intial conditions
34 pc0   = 13;
35 pp0   = 208;
36 qbit0 = 3000/60000;
37 zc0   = 0.5;
38 pbit0 = 470;
39 pcref0 = 13;
40 hmud0 = 3000;
41 qbck0 = 235/60000;
42 qp0   = 3000/60000;
43 hpipe0 = 3000;
44 qc0   = qp0+qbck0;
45
46 % storage arrays
47 pc    = zeros(length(time),1);
48 pp    = zeros(length(time),1);
49 qbit  = zeros(length(time),1);
50 qbck  = zeros(length(time),1);
51 qp    = zeros(length(time),1);
52 zc    = zeros(length(time),1);
53 pbit  = zeros(length(time),1);
54 pcref = zeros(length(time),1);
55 hmud  = zeros(length(time),1);
56 qc    = zeros(length(time),1);
57 hpipe = zeros(length(time),1);
58

```

```

59 pc(1) = pc0;
60 pp(1) = pp0;
61 qbit(1) = qbit0;
62 zc(1) = zc0;
63 pbit(1) = pbit0;
64 pcref(1) = pcref0;
65 hmud(1) = hmud0;
66 qbck(1) = qbck0;
67 qp(1) = qp0;
68 hpipe(1) = hpipe0;
69 qc(1) = qc0;
70
71 %PI controller to keep pbit at a setpoint
72 pbitref = 470;
73 Kppcref = 4;
74 Kipcref = 10;
75 eipcref = pcref0/Kipcref;
76
77 %PI controller to keep pc at a setpoint
78 Kp = 0.01;
79 Ki = 5e-3;
80 ei = zc0/Ki;
81
82 %PI controller to keep zc at a setpoint
83 zcref = 0.5;
84 Kpbck = 0.01;
85 Kibck = 0.005;
86 eibck = qbck0/Kibck;
87
88 %PI controller to keep qp at a setpoint
89 qpref = 3000/60000;
90 Kppp = 0.1;
91 Kiqp = 0.1;
92 eiqp = qp0/Kiqp;
93
94 %PI controller to keep hpipe at a setpoint
95 hpiperef = 3000;
96 Kphpipe = 0.1;
97 Kihpipe = 0.5;
98 eihpipe = hpipe0/Kihpipe;
99
100 %Euler integration
101 for i=1:length(time)-1
102     %Define current state vectors
103     x = [pc(i); pp(i);qbit(i)];
104
105     %Set inputs
106     if time(i)<100
107         qpref = 3000/60000;
108         hpiperef = 3000;
109     elseif time(i)<200
110         %Ramp down pump
111         qpref = 0;
112         zcref = 0.15;
113     elseif time(i)<300
114         %Trip out drill string
115         hpiperef = 2973;
116     elseif time(i)<400
117         %Trip in drill string
118         hpiperef = 3000;
119     elseif time(i)≥400

```

```

120     %Ramp up pump
121     qpref = 3000/60000;
122     zcref = 0.5;
123 end
124
125 %Controllers
126 if i ≥ 2
127
128     %Cascade controller to keep pbit at setpoint by changing pcref
129     epcref = pbitref - pbit(i-1);
130     eipcref = eipcref + dT*epcref;
131     pcref(i) = max(Kppcref*epcref + Kipcref*eipcref,0);
132
133     %Controller to keep qp at setpoint, with switch
134     eqp = qpref - qp(i-1);
135     eiqp = eiqp + dT*eqp;
136     if abs(epcref) < 5
137         qp(i) = Kpqp*eqp + Kiqp*eiqp;
138     else
139         qp(i) = qp(i-1);
140     end
141
142     %Controller to keep hpipe at setpoint, with switch
143     ehpipe = hpipe - hpipe(i-1);
144     eihpipe = eihpipe + dT*ehpipe;
145     if abs(epcref) < 5
146         hpipe(i) = Kphpipe*ehpipe + Kihpipe*eihpipe;
147     else
148         hpipe(i) = hpipe(i-1);
149     end
150
151     %Simple controller to keep pc at pcref by changing zc
152     e = pc(i-1)-pcref(i-1);
153     ei = ei + dT*e;
154     zc(i) = min(max(Kp * e + Ki * ei,0),100);
155
156     %Input reset controller to keep zc at setpoint by changing qbck
157     ebck = zcref - zc(i-1);
158     eibck = eibck + dT*ebck;
159     qbck(i) = max( Kpbck*ebck + Kibck*eibck,0);
160
161 end
162
163
164 %Calculate right-hand side
165 [f qccalc] = calcf(time(i), x, zc(i), qbck(i), qp(i), hBit, Va, ...
166     VaDot, Vd, betaa, betad, M, theta1, theta2, rhod, rhoa, g);
167
168 %Step states
169 x = x + dT*f;
170
171 if i>2
172     vpipe = (hpipe(i)-hpipe(i-1))/dT;
173 else
174     vpipe = 0;
175 end
176
177 qc(i+1) = qccalc + Apipe*vpipe;
178 hmud(i+1) = hmud(i)+Apipe*vpipe/Atot*dT + (qp(i) + qbck(i) -...
179     qc(i))/Atot*dT;
180

```

```

181     %Store results
182
183     pc(i+1) = x(1);
184     pp(i+1) = x(2);
185     qbit(i+1) = x(3);
186
187     %Calculate pbit
188     pbit(i+1) = pc(i+1)+theta1*qbit(i+1)+rhoa*g*hBit;
189
190 end
191
192 %Store last results
193 zc(length(time)) = zc(length(time)-1);
194 qp(length(time)) = qp(length(time)-1);
195 qbck(length(time)) = qbck(length(time)-1);
196 pceref(length(time)-1:length(time)) = pceref(length(time)-2);
197 hmud(length(time)) = hmud(length(time)-1);
198 hpipe(length(time)) = hpipe(length(time)-1);
199 qc(length(time)) = qc(length(time)-1);
200
201 %% Plot results
202 set(0, 'defaultaxesfontsize',14);
203 set(0, 'defaulttextfontsize',14);
204 set(0, 'DefaultLineLineWidth',1.5);
205 set(0, 'DefaultFigureColor', 'none');
206 legFontSize = 16;
207 scrsz = get(0, 'ScreenSize');
208
209 figure('Position',[1 scrsz(4)/2 scrsz(3)/2 scrsz(4)/2])
210 plot(time,pc,time,pceref,time,pbit-400)
211 h(1)=legend('$p_c$', '$p_{c,s}$', '$p_{bit}$ - 400', 'Location', 'Best');
212 xlabel('Time [s]');
213 ylabel('Pressure [bar]')
214 set(h, 'Interpreter', 'latex', 'FontSize', legFontSize)
215 set(gcf, 'PaperPositionMode', 'auto') % Use screen size
216 print -djpeg cascadecontrol
217
218 figure('Position',[1 scrsz(4)/2 scrsz(3)/2 scrsz(4)/2])
219 plot(time,zc*100)
220 h(1)=legend('$z_c$');
221 axis([0 600 0 100]);
222 ylabel('Valve Position [%]');
223 xlabel('Time [s]');
224 set(h, 'Interpreter', 'latex', 'FontSize', legFontSize)
225 set(gcf, 'PaperPositionMode', 'auto') % Use screen size
226 print -djpeg cascadecontrol2
227
228
229 figure('Position',[1 scrsz(4)/2 scrsz(3)/2 scrsz(4)/2])
230 plot(time,qp*60000,time,qbit*60000)
231 h(1)=legend('$q_p$', '$q_{bit}$', 'Location', 'Best');
232 %axis([0 600 0 2500]);
233 ylabel('Volume flow [liter/min]');
234 xlabel('Time [s]');
235 set(h, 'Interpreter', 'latex', 'FontSize', legFontSize)
236 set(gcf, 'PaperPositionMode', 'auto') % Use screen size
237 print -djpeg cascadecontrol3
238
239 figure('Position',[1 scrsz(4)/2 scrsz(3)/2 scrsz(4)/2])
240 plot(time,qbck*60000,time,qc*60000)
241 h(1)=legend('$q_{bck}$', '$q_c$', 'Location', 'Best');

```

```

242 axis([0 600 0 6000]);
243 ylabel('Volume flow [liter/min]');
244 xlabel('Time [s]');
245 set(h,'Interpreter','latex','FontSize',legFontSize)
246 set(gcf,'PaperPositionMode','auto') % Use screen size
247 print -djpeg cascadecontrol4
248
249 figure('Position',[1 scrsz(4)/2 scrsz(3)/2 scrsz(4)/2])
250 plot(time,-hpipe)
251 h(1)=legend('$h_{bit}$');
252 %axis([0 600 -3010 -2960]);
253 xlabel('Time [s]');
254 ylabel('Height [m]')
255 set(h,'Interpreter','latex','FontSize',legFontSize)
256 set(gcf,'PaperPositionMode','auto') % Use screen size
257 print -djpeg cascadecontrol5
258
259 figure('Position',[1 scrsz(4)/2 scrsz(3)/2 scrsz(4)/2])
260 plot(time,pbit)
261 h(1)=legend('$p_{bh}$');
262 %axis([0 600 -3010 -2960]);
263 xlabel('Time [s]');
264 ylabel('Pressure [bar]')
265 set(h,'Interpreter','latex','FontSize',legFontSize)
266 set(gcf,'PaperPositionMode','auto') % Use screen size
267 print -djpeg cascadecontrol6

```

calcf.m:

```

1 function [f qc] = calcf(t,x,zc,qbck,qp,hBit,Va,VaDot,Vd,betaa,betad,M,...
2     theta1,theta2,rhod,rhoa,g)
3 %Function calculates right hand side f = [f1;f2;f3] of system equations
4 %x = [pc;pp;qbit]
5 %?NS - 2009
6 %Modified: DEH - 2010
7
8 % get states
9 pc = x(1);
10 pp = x(2);
11 qbck = x(3);
12
13 % calc qc
14 qc = 0.0025*zc*sqrt(2/rhoa*(pc-0));
15
16 % calc f
17 f1 = (betaa/Va) * (qbck - qc + qbck + VaDot);
18 f2 = (betad/Vd) * (qp - qbck);
19
20 % project
21 if qbck>0
22     f3 = (1/M) * (pp-pc-theta1*qbit-theta2*abs(qbit)*qbit +...
23         (rhod-rhoa)*g*hBit);
24 else
25     f3 = max((1/M) * (pp-pc+(rhod-rhoa)*g*hBit),0);
26 end
27
28 f = [f1;f2;f3];
29 end

```